Geophys. J. Int. (1996) **124**, 935–953

Palaeomagnetism and magnetostratigraphy of Triassic strata in the Sangre de Cristo Mountains and Tucumcari Basin, New Mexico, USA

Roberto S. Molina-Garza,[1] John W. Geissman,[1] Spencer G. Lucas[2] and Rob Van der Voo[3]

[1] *Department of Earth and Planetary Sciences, University of New Mexico, Albuquerque, NM, 87131-1116, USA*

[2] *New Mexico Museum of Natural History and Science, 1810 Mountain Road NW, Albuquerque, NM, 87104, USA*

[3] *Department of Geological Sciences, University of Michigan, Ann Arbor, MI, 48109-1063, USA*

Accepted 1995 October 18. Received 1995 October 10; in original form 1995 February 16

SUMMARY

We report palaeomagnetic data and a composite magnetic polarity sequence for Middle and Upper Triassic rocks assigned to the Anton Chico Member of the Moenkopi Formation and Chinle Group, respectively, exposed along the eastern flank of the Sangre de Cristo Mountains and in the Tucumcari Basin of eastern and northeastern New Mexico. Thermal demagnetization isolates a well-defined, dual polarity, characteristic magnetization, carried in most cases by haematite and interpreted as an early acquired chemical remanent magnetization (CRM). Characteristic magnetizations from 74 palaeomagnetic sites (one site = one bed) are used to define a magnetic polarity sequence, which we correlate with previously published Triassic data obtained from both marine and non-marine rocks. Preliminary correlation suggests that the resolution of magnetostratigraphic data derived from continental strata is not necessarily of lesser quality than that from marine rocks. On the basis of the magnetostratigraphic data, a profound unconformity is believed to separate lower–middle Norian and upper Norian–Rhaetian strata of the Chinle Group. Palaeomagnetic poles derived from selected sites in steeply dipping (> 85°) strata for the Middle Triassic (Anisian, ~240 Ma: 50°N 121°E; $N = 8$), late Carnian–early Norian (~225 Ma: 53°N 104°E; $N = 16$), and late Norian–Rhaetian (~208 Ma: 59°N 77°E; $N = 8$) are in relatively good agreement with previously published data for the Moenkopi Formation and Chinle Group and related strata in southwest North America. None the less, comparison with palaeomagnetic poles obtained from gently dipping or flat-lying Triassic strata from this study (Anisian, 46°N 112°E; $N = 13$; late Carnian, 54°N 87°E; $N = 12$) and previously published Triassic poles in southwest North America suggest that a modest 'apparent rotation' not greater than about 5° affects declinations from steeply dipping rocks. The distribution of palaeomagnetic poles indicates ~25° (angular distance) of apparent polar wander between about 240 and 208 Ma.

Key words: magnetostratigraphy, New Mexico, palaeomagnetism, sediments, Triassic.

INTRODUCTION

Extending the magnetic polarity sequence to the early Mesozoic and Palaeozoic requires palaeomagnetic sampling of strata now exposed on the continents. The magnetic polarity record derived from stratigraphic sequences can, in principle, provide as good a resolution as the late Mesozoic and Cenozoic sea-floor record (e.g. Lowrie *et al.* 1982). Thus far, acquisition of polarity data for Triassic and older rocks has been hampered for several reasons, including the lack of attention to numerous stratigraphic sequences, absence of primary magnetizations, and inadequate bio- or chronostratigraphic control. The importance of extending the magnetic polarity time scale to the early Mesozoic and late Palaeozoic cannot be overstated. Magnetostratigraphy is an invaluable tool for global and regional correlation of strata as well as geological events of global significance, such as mass extinctions. Furthermore, studies of long-term changes in the frequency of polarity reversals provide important information for the dynamo

theories and the time-scales associated with core–mantle interactions.

Recent efforts to extend the magnetic polarity time-scale into the Permian and Triassic have focused on palaeontologically well-characterized rocks (dated by ammonoids and/or conodonts), and links to the Triassic time-scale are relatively straightforward. Tethyan pelagic marine sections (Muttoni & Kent 1994; Muttoni *et al.* 1994; Gallet *et al.* 1992, 1993, 1994) have provided a detailed magnetostratigraphy for parts of the Middle and Late Triassic. Similarly, magnetostratigraphic data are available for rocks in the Canadian Arctic Archipelago proposed as stratotypes defining the Early Triassic stages (Ogg & Steiner 1991), and high-resolution data have been published for proposed Permo-Triassic boundary sections in Sichuan Province in southern China and the Nammal Gorge in Pakistan (Steiner *et al.* 1989; Heller *et al.* 1988; Haag & Heller 1991).

Magnetostratigraphic data have been available for non-marine Permian and Triassic rocks for some time (Picard 1964; McMahon & Strangway 1968; Helsley 1969; Helsley & Steiner 1974; Reeve & Helsley 1972). Usually, temporal resolution of non-marine sequences is low, and correlation with the geological time-scale is difficult. The reliability of magnetostratigraphic records from redbeds has also been controversial (Larson *et al.* 1982). Recent magnetic polarity studies for the Early and Middle Triassic from redbeds in western and southwestern North America (Shive, Steiner & Huycke 1984; Molina-Garza *et al.* 1991; Steiner, Morales & Shoemaker 1993) suggest that relatively reliable records of short-duration polarity intervals have been observed, in turn suggesting that reliable magnetostratigraphic data may be recoverable from non-marine strata. Recent studies, however, have faced problems similar to those of early workers: temporal resolution is poor and biostratigraphic data scarce. Continuous coring of continental rift deposits of the Newark Supergroup in the Newark Basin has provided the most detailed Late Triassic data in non-marine strata (Kent, Witte & Olsen 1995). Data from the Newark basin can be linked to the Triassic time-scale via radiometric dating and an interpreted astronomically calibrated cyclostratigraphy (Van Houten 1962; Olsen 1986).

To establish the Late Triassic magnetic polarity sequence as recorded in the Chinle Group and related strata of southwestern North America, we obtained palaeomagnetic and magnetostratigraphic data for non-marine Triassic strata from the southern end of the Sangre de Cristo Mountains and from the Tucumcari Basin of northeastern and eastern New Mexico. Preliminary results of the magnetostratigraphic correlation within the Chinle Group were published in Molina-Garza, Geissman & Lucas (1993). The recent availability of magnetostratigraphic data from well-dated Upper Triassic marine and non-marine sequences and improved temporal resolution of the biostratigraphy of the Chinle Group (e.g. Lucas 1993) provide an opportunity to establish a Late Triassic magnetic polarity time-scale and to examine the related problem of correlation of the marine and non-marine biochronologies. Palaeomagnetic and magnetostratigraphic data have been previously published for flat-lying Triassic strata in the Tucumcari basin of eastern New Mexico: the Middle Triassic Anton Chico Member of the Moenkopi Formation (Steiner & Lucas 1992); and the Upper Triassic Bull Canyon (formerly upper shale member) and Redonda Formations of the Chinle Group (Bazard & Butler 1991; Reeve & Helsley 1972). The data presented here provide a refined structure and calibration of the North American apparent polar wander path (APWP).

GEOLOGY AND SAMPLING

Triassic non-marine strata are exposed along the eastern Sangre de Cristo uplift in a narrow and discontinuous north–south trending belt extending from the Colorado–New Mexico line to south of Las Vegas, New Mexico (Fig. 1). Equivalent strata are widespread in eastern New Mexico (the Tucumcari basin and the drainage of the Pecos and Canadian rivers). These rocks have been assigned, in ascending stratigraphic order, to the Middle Triassic Anton Chico Member of the Moenkopi Formation, and the Upper Triassic Santa Rosa, Garita Creek, Trujillo, Bull Canyon, and Redonda Formations, all of which are included in the Chinle Group (Lucas & Hunt 1987; Lucas & Hunt 1989; Lucas 1993). Correlation of Upper Triassic strata exposed in the Sangre de Cristo Mountains with Triassic strata exposed in the Tucumcari basin is based on relatively unambiguous lithological characteristics and homotaxis (Lucas, Hunt & Huber 1990). The stratigraphic nomenclature of Upper Triassic strata in eastern New Mexico is summarized in Fig. 2. This figure also shows correlation of these strata with Upper Triassic rocks on the Colorado Plateau, west Texas and central New Mexico (after Lucas 1993).

The Anton Chico Member of the Moenkopi Formation rests disconformably on Permian strata of the Artesia Group. The Anton Chico Member is dominated by greyish-red, trough-crossbedded litharenites and lithic wackes with lesser amounts of mudstone and siltstone. These strata have been correlated with the Holbrook Member of the Moenkopi Formation in western New Mexico and eastern Arizona, and the early Anisian age is well established by the presence of the index taxon *Eocyclotosaurus*, a capitosauroid amphibian (Lucas & Morales 1985; Morales 1987, 1993). The upper Carnian Santa Rosa Formation overlies a thin package of 'mottled strata', pedogenically altered beds that commonly define the base of the Chinle Group on the Colorado Plateau (Stewart, Poole & Wilson 1972). The Santa Rosa Formation of the Tucumcari basin includes three members, also recognized in the Sangre de Cristo Mountains. The Tecolotito Member contains mostly yellowish-grey and olive-grey trough-crossbedded quartzarenite and minor amounts of conglomerate. The Tecolotito Member is overlain by variegated mudstone of the Los Esteros Member, which in turn underlies quartzarenites of the Tres Lagunas Member. Mudstone-dominated strata that overlie the Tres Lagunas Member have been assigned to the Garita Creek Formation. Mudstone is typically greyish-red, purple, reddish-brown and bentonitic. The Trujillo Formation disconformably overlies strata of the Garita Creek and is characterized by relatively thick, resistant, greyish-yellow-green, fine–medium grained, well sorted, trough-crossbedded quartzarenites, with minor siltstone and intra-formational conglomerate. The Bull Canyon and Redonda Formations are mudstone dominated. They typically contain thin sandstone sheets within reddish-brown and greyish-red siltstone and mudstone.

Upper Triassic strata in the Sangre de Cristo Mountains lack age-diagnostic fossils, thus age determinations are based on non-marine vertebrate fossils, macrofossil plants and palynostratigraphy of the Chinle Group in eastern New Mexico. The Chinle Group provides the most complete biochronology of the non-marine Upper Triassic (Lucas 1993; 1995).

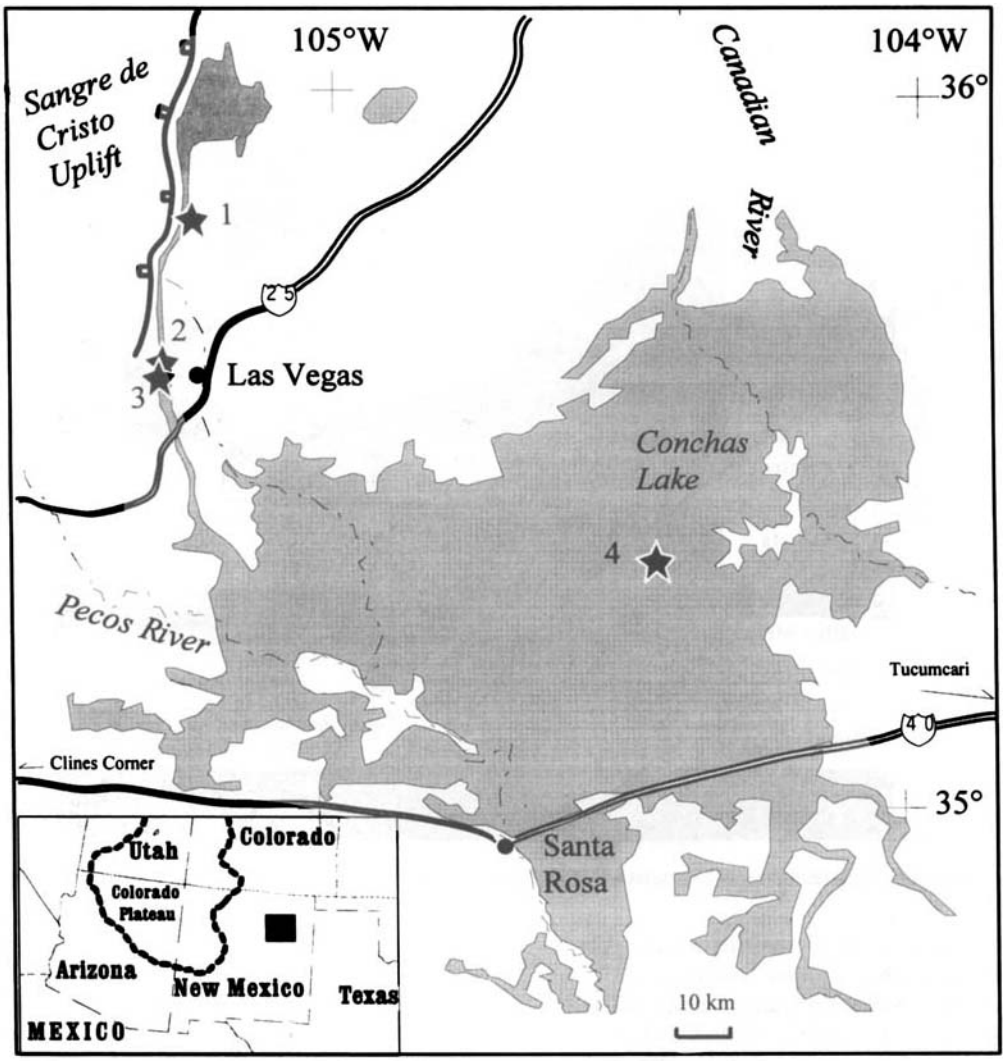

Figure 1. Simplified outcrop map of Triassic strata (stippled) in the Tucumcari basin and surrounding areas of eastern New Mexico. Sampling localities (stars) are (1) La Cueva, (2) San Sebastian Canyon, (3) Montezuma Gap and (4) Garita Creek.

Relatively good temporal resolution is based on a succession of four distinct tetrapod faunas (mostly phytosaurs and aetosaurs) designated 'faunachrons' A to D by Lucas (1993) and named by Lucas & Hunt (1993; Fig. 2). A late Carnian age (Tuvalian) for the base of the Santa Rosa Formation (Otischalkian faunachron) is indicated by the primitive phytosaur *Paleorhinus* (Hunt & Lucas 1991). The contact between the Santa Rosa and Garita Creek formations is conformable. The upper members of Santa Rosa Formation and the Garita Creek Formation are also late Carnian. Lucas (1993) assigns these strata to the Adamanian faunachron. They are included in the Dinophyton floral zone of Ash (1980) and correlated with the lower Petrified Forest Formation of the Colorado Plateau. The late Carnian–early Norian age of the Trujillo Formation is based on vertebrate fauna of the Revueltian faunachron (Lucas & Hunt 1989; Lucas 1993), fossil plants restricted to the *Dinophyton* zone of Ash (1980), and palynomorphs belonging to the New Oxford–Lockatong palynozone of the Newark Supergroup (Cornet 1993). The Bull Canyon Formation (originally upper shale member of the Chinle Formation) conformably overlies the Trujillo beds and is also of Revueltian faunachron age. It contains a rich fossil-vertebrate fauna assigned to the early Norian (Lucas 1990; Lucas & Hunt 1989). Age-equivalent strata in western New Mexico and eastern Arizona include the Painted Desert Member and Correo Sandstone of the Petrified Forest Formation. Dinosaur-rich faunas in the Redonda Formation, as well as more evolutionary advanced phytosaur fossils than those observed in the Bull Canyon Formation, suggest a late Norian–Rhaetian age (Apachean faunachron) for the Redonda Formation (Lucas 1990; Lucas & Hunt 1993). Two intra-Chinle Group unconformities separate upper Carnian–lower Norian strata, and early–middle Norian–late Norian–Rhaetian strata, respectively (Fig. 2).

26 palaeomagnetic sites were collected from the Anton Chico Member at localities in Montezuma Gap (35.56°N 105.27°W; along New Mexico Highway 65) and La Cueva (35.92°N 105.25°W; along New Mexico Highway 3; Fig. 1). At Montezuma Gap we also collected three sites from the upper beds of the Upper Permian (Guadalupian) Artesia Group. The Upper Triassic section was sampled at Montezuma Gap and San Sebastian Canyon (35.66°N 105.28°W; 34 sites approximately 1.5 km north of Highway 65, and one site in the Jurassic Entrada Formation). The Garita Creek Formation was

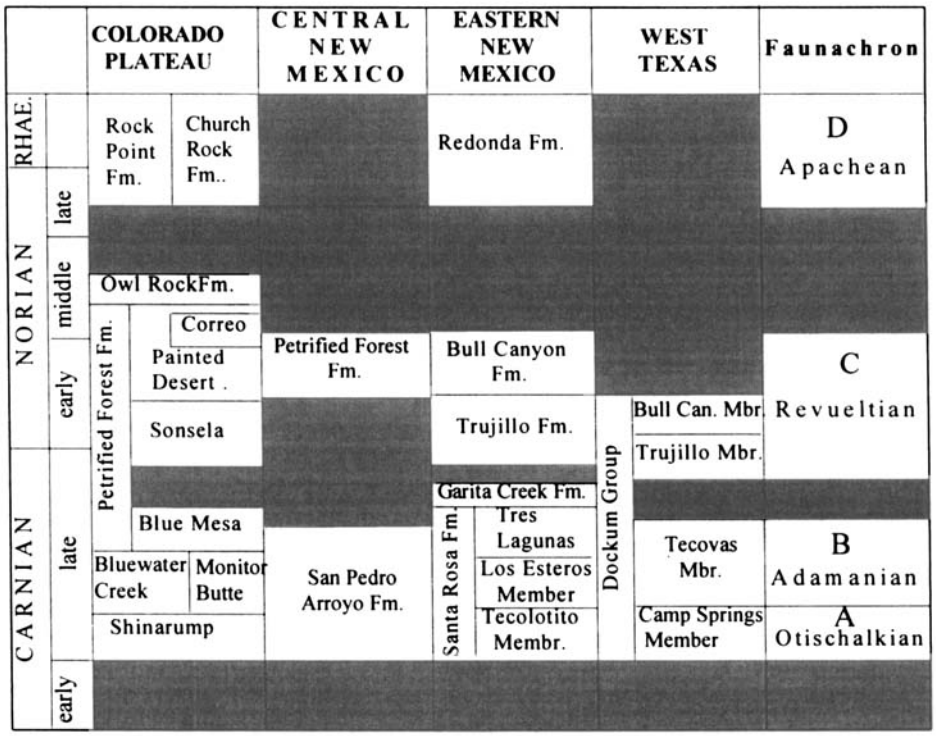

Figure 2. Simplified stratigraphic nomenclature and correlation of the Upper Triassic Chinle Group of southwestern North America.

sampled at its type locality in the Tucumcari basin (35.29°N 104.40°W; 17 sites along New Mexico Highway 405). At Montezuma Gap and San Sebastian Canyon strata strike to the north and dip steeply (>85°). Sites collected at La Cueva are from gently east-dipping Anton Chico strata (dips ~40°), whereas the Garita Creek Formation is horizontal at its type locality. A great majority of the sites were collected from individual sandstone or siltstone beds between a few and tens of centimetres in thickness. Sites at the base of the Trujillo Formation comprise samples collected transversely from as many as three thick (~1 m) adjacent sandstone beds. Mudstone intervals were sparsely sampled because they are not suitable for drilling and are poorly exposed. Schematic stratigraphic sections with palaeomagnetic sites are illustrated in Fig. 3. The sections overlap and yield a near-complete stratigraphic record of the Triassic in this area. The largest stratigraphic gaps are within the Bull Canyon and Redonda Formations. Samples were drilled as standard 2.5 cm diameter cores and oriented using a clinometer and a magnetic compass; orientations were verified with a sun compass where possible. In the laboratory one or more 2.1 cm long specimens were cut from each sample.

PALAEOMAGNETIC ANALYSIS

The natural remanent magnetization (NRM) of the samples collected at Montezuma Gap was measured on a two-axis ScT cryogenic magnetometer at the University of Michigan; a three-axis 2G Enterprises cryogenic magnetometer at the University of New Mexico was used for the rest of the collection. Samples were subjected to progressive thermal or alternating field (AF) demagnetization. Thermal demagnetization proved more capable in isolating the characteristic remanence, but a few specimens from selected sites were demagnetized using alternating fields. Thermal demagnetization of pilot samples (typically two per site) was carried out in up to 24 steps; abbreviated sequences of six to 12 steps were used in the rest of the samples. The vectorial composition of the NRM was interpreted from inspection of orthogonal demagnetization diagrams (Zijderveld 1967). Directions of magnetization components were calculated using principal component analysis (PCA) methods (Kirschvink 1980).

Samples are characterized by moderate magnetic moments per unit volume, of the order of 10^{-4} to 10^{-2} A m^{-1}. Typical demagnetization diagrams are depicted in Figs 4 to 6. In most samples a south-southeast- or north-northwest-directed shallow magnetization is isolated at temperatures above 600 °C. This magnetization is interpreted as the characteristic magnetization (ChRM). A north-directed and moderately steep positive magnetization commonly overprints the ChRM. Results obtained from each formation are discussed in detail below.

Anton Chico Member

Most Anton Chico sites were collected in very fine-grained, light reddish-brown or purplish-brown, silty sandstone. Their behaviour upon thermal demagnetization is relatively straightforward. A great majority of the samples exhibit one or two components of magnetization (Figs 4a and b). The first component is unblocked below about 550 °C and comprises about

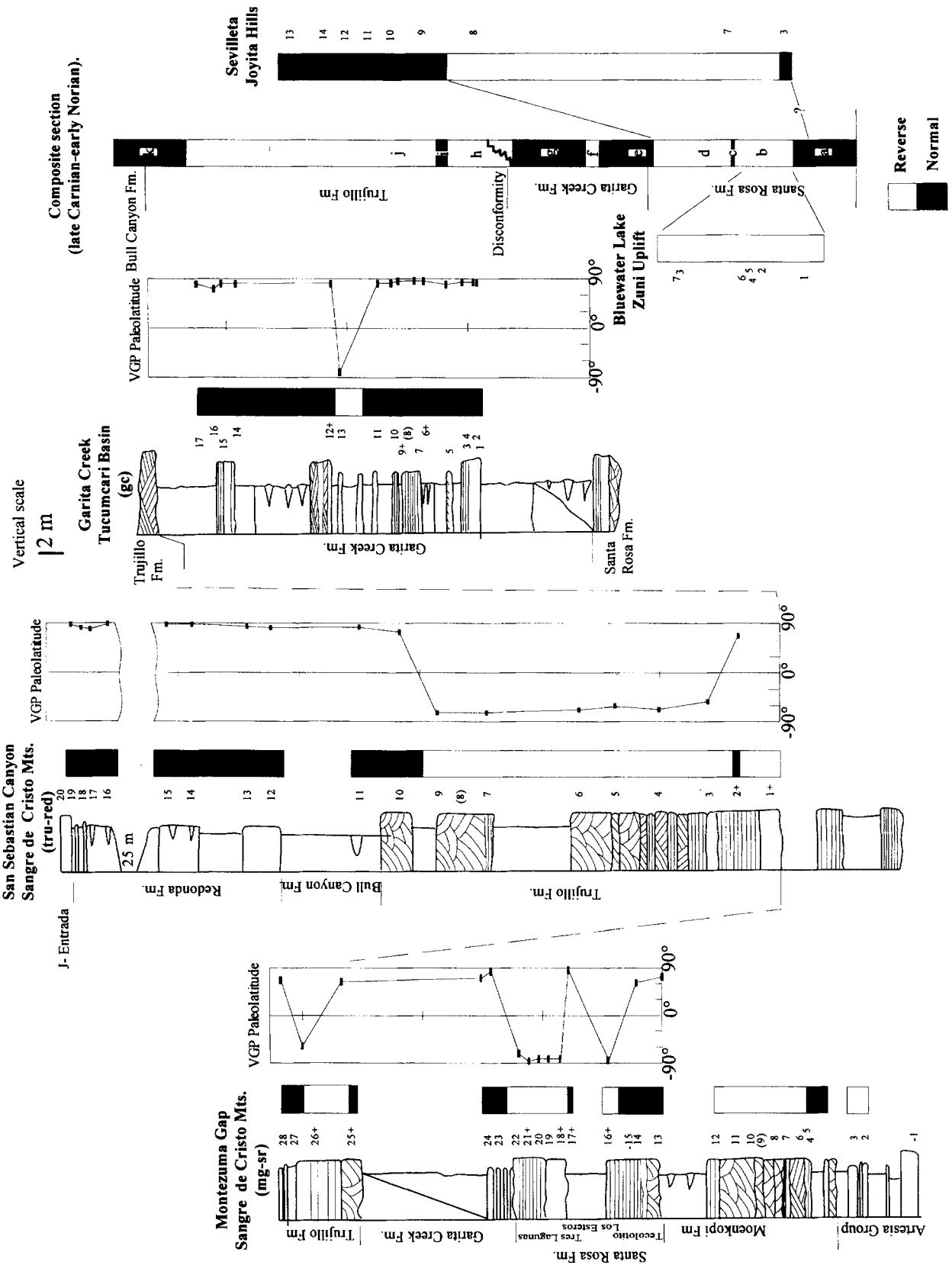

Figure 3. Schematic stratigraphic sections of Upper Triassic strata at Montezuma Gap, San Sebastian Canyon and Garita Creek showing the distribution of palaeomagnetic sampling sites. Sites in parentheses were not demagnetized; sites modified by a '+' sign were excluded from pole calculations but were used for polarity determinations. A composite magnetostratigraphic sequence includes data from central and western New Mexico. Polarity intervals are labeled 'a' through 'k'. We also plot VGP paleolatitudes for individual sites.

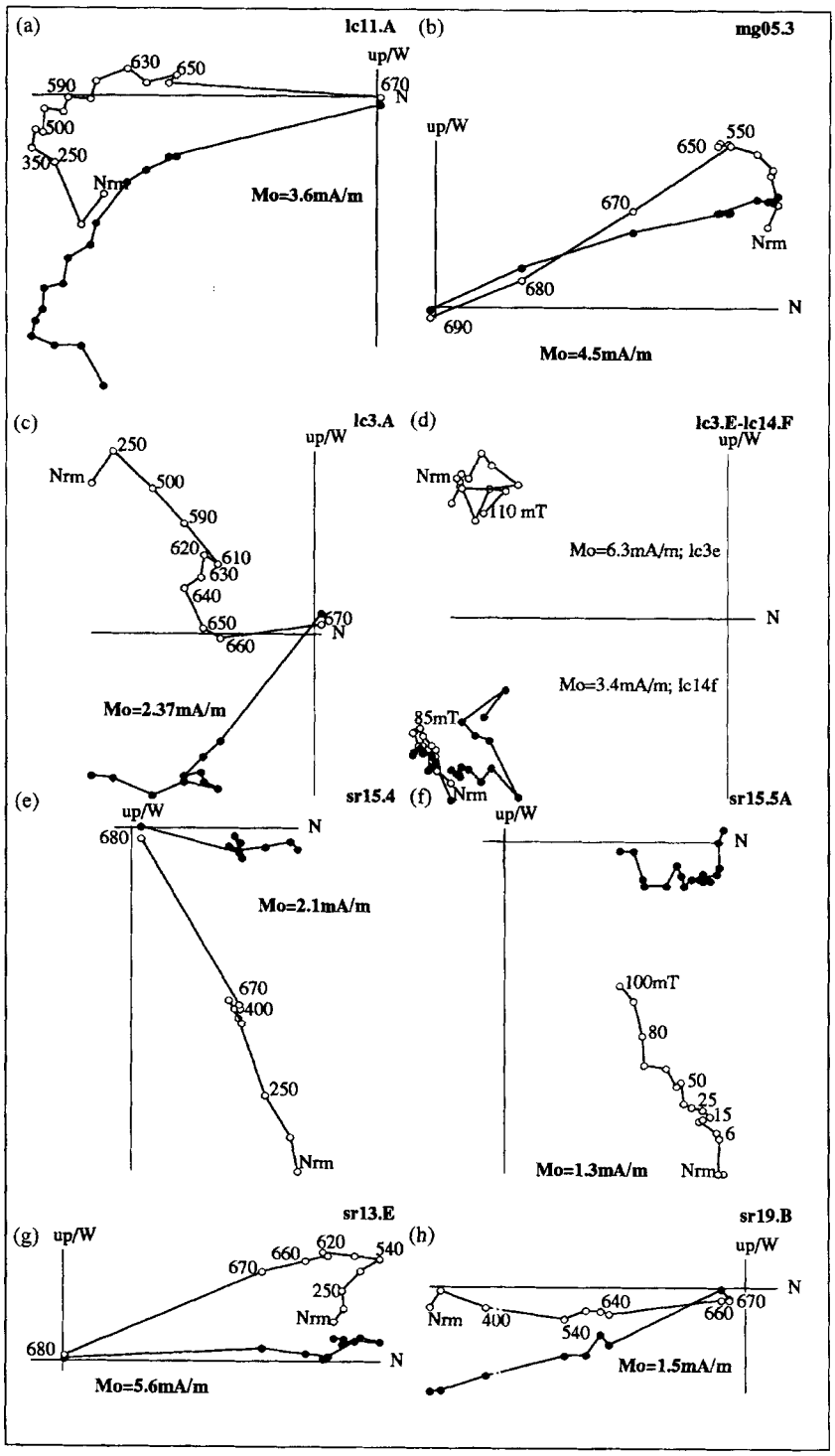

Figure 4. Orthogonal demagnetization diagrams (Zijderveld 1967) of specimens of the Anton Chico Member of the Moenkopi Formation (a–d) and Santa Rosa Formation (e–h). All diagrams plotted in *in situ* coordinates except for c. Open/closed symbols are projections in the vertical/horizontal plane. Mo = initial magnetization.

20 per cent of the NRM. It has a predominantly steep positive inclination (*in situ*), with somewhat variable declination, although north- to northeast-directed declinations are most common. The ChRM is characterized by predominantly southeast-directed shallow directions (Fig. 4a). Directions of opposite polarity (northwest and shallow) are observed at two sites from the Montezuma Gap section (Fig. 4b). The ChRM of the Anton Chico is well defined; linear segments directed to the origin have maximum angular deviation (MAD) values less than about 5°. The ChRM unblocks over a narrow range of temperatures between 620 and 690 °C.

Some samples, mainly from the La Cueva section, are

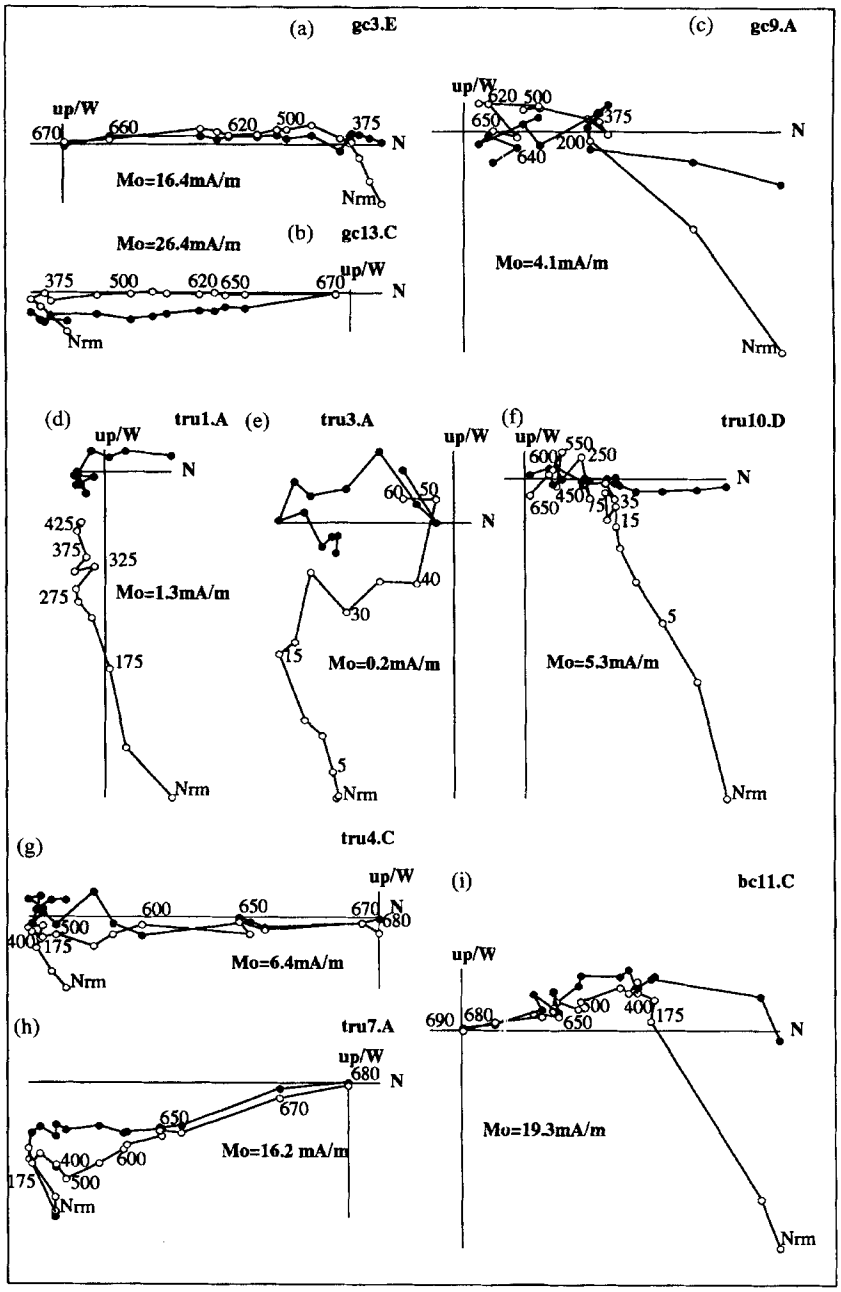

Figure 5. Orthogonal demagnetization diagrams (Zijderveld 1967) of specimens of the Garita Creek (a–c), Trujillo (d–h) and Bull Canyon Formations (i). All diagrams plotted in *in situ* coordinates. Open/closed symbols are projections in the vertical/horizontal plane.

characterized by a relatively ill-defined magnetization component (MAD angles of about 10–15°) with high coercivities (>100 mT) and unblocking temperatures between 500 and 650 °C. This component has (tilt corrected) steep negative inclination and southeast-directed declination (Fig. 4c). The high resistance to AF demagnetization (Fig. 4d) indicates that the ChRM and the steep negative south-directed overprint are carried by haematite. IRM (isothermal remanent magnetization) acquisition and demagnetization indicate that contributions from a low coercivity phase to the magnetic mineralogy of Anton Chico sandstones are minor, with about 80 per cent of the saturation IRM (using a 3 T induction) remaining after AF demagnetization to 120 mT (Fig. 7a).

Santa Rosa Formation

Typical demagnetization diagrams for specimens of the Santa Rosa Formation are depicted in Fig. 4. Demagnetization behaviour of NRM is more variable than in the Anton Chico Formation. Coarse-grained specimens of the Tecolotito Member are mostly characterized by univectorial magnetizations carried by both magnetite and haematite with (*in situ*) north-directed declinations and steep positive inclinations (Figs 4e and f). This magnetization is interpreted as an overprint of recent origin. The ChRM of the Santa Rosa Formation (north- or south-directed and shallow) was isolated in reddish-grey fine-grained rocks. Magnetizations of dual polarity and inter-

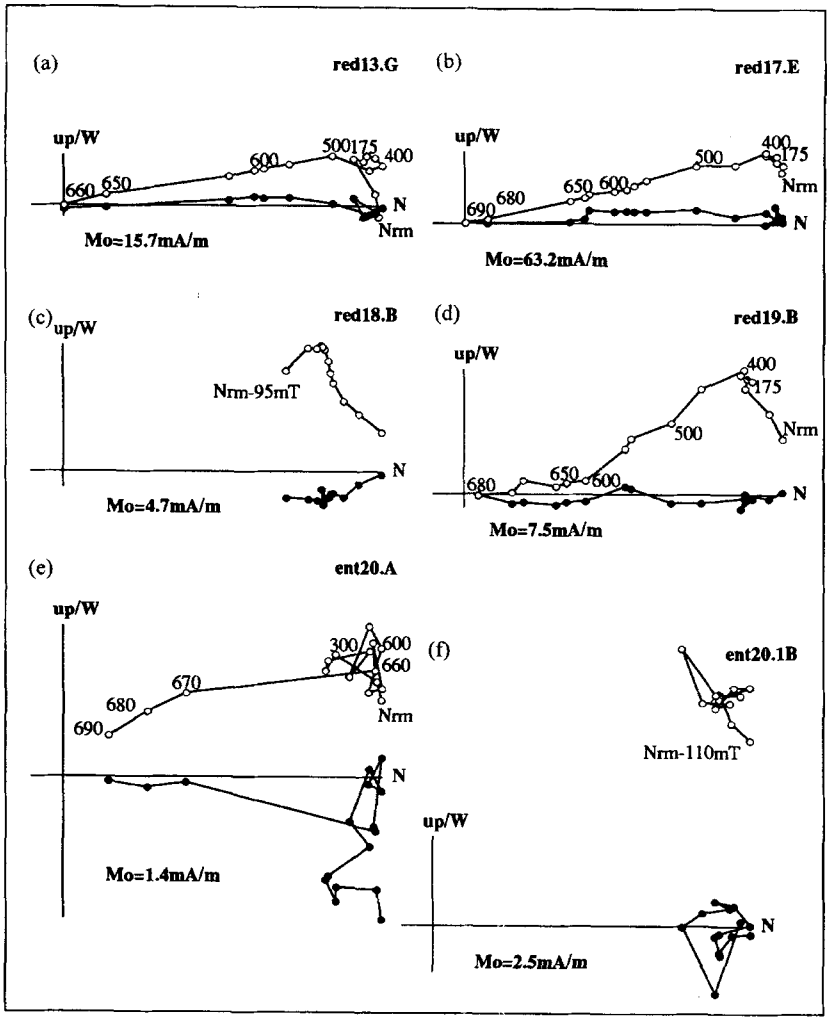

Figure 6. Orthogonal demagnetization diagrams (Zijderveld 1967) of specimens of the Redonda (a–d) and Entrada (e and f) Formations. All diagrams plotted in *in situ* coordinates. Open/closed symbols are projections in the vertical/horizontal plane.

preted to be primary have typically distributed laboratory unblocking temperatures between 400 and 680 °C (Figs 4g and h), with samples in the Tres Lagunas Member showing a narrow range of unblocking temperatures above ~620 °C. A high contribution of a cubic phase (magnetite or maghemite) to the magnetic mineralogy of the Santa Rosa samples is suggested by median destructive fields for the saturation remanence IRM near or below 100 mT; also, a large percentage (30 to 90 per cent) of the total IRM is induced by 0.3 T (Fig. 7b).

Garita Creek Formation

Sites in the Garita Creek Formation were collected from fine-grained reddish-brown siltstone and sandstone. These samples exhibit two general behaviours. Well-behaved sites are characterized by a north-directed and shallow magnetization (south directed and shallow at one site) unblocked between about 400 and 680 °C (Figs 5a and b). This magnetization is considered the characteristic magnetization and is partially overprinted by a small north-directed and steep positive magnetization that is removed below about 200 °C. The low unblocking temperature component is well defined in sites of the second group, which includes samples of medium-grained to conglomeratic sandstones consisting of pebble-size clasts of siltstone and mudstone. In sites 6, 8, 9 and 12 the ChRM cannot be estimated with sufficient confidence (Fig. 5c), because most of the NRM remains after heating to 400 °C but the magnetization does not decay linearly to the origin (typical MAD values for directions calculated by PCA are greater that about 15°). Sites with this kind of behaviour were thus excluded from pole calculations. The polarity at these sites, however, is unambiguous and is also supported by the data from immediately adjacent beds. IRM acquisition and demagnetization suggest that contributions from a cubic phase to the IRM are small, no more than 25 per cent of the IRM is induced with 0.3 T and the IRM is highly resistant to AF demagnetization (Fig. 7b).

Trujillo Formation

The lower 10 m of the Trujillo Formation (sites tru1 to tru3 and tru25 to tru26) are mostly characterized by thick, typically non-haematitic, coarse- to medium-grained sandstone beds that generally do not respond to AF or thermal demagnetiz-

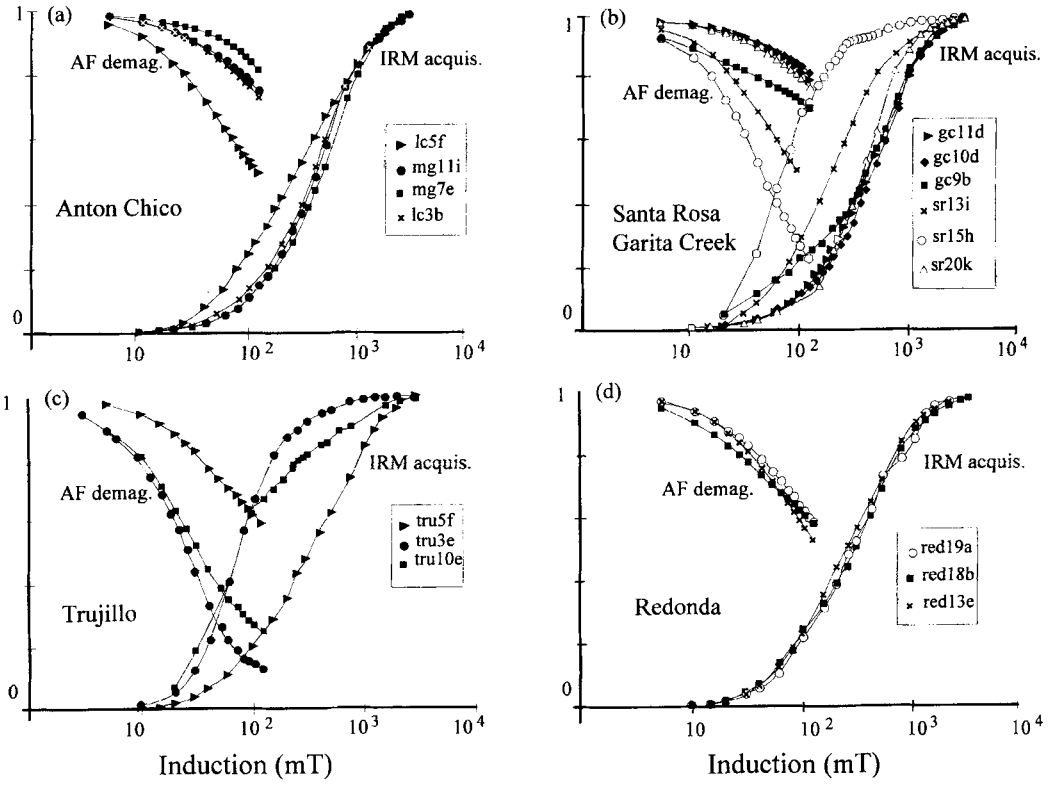

Figure 7. Normalized IRM acquisition and AF demagnetization of the saturation remanence IRM for selected specimens.

ation. Some samples are characterized by a low-unblocking-temperature component in the direction of the recent dipole field (Fig. 5d); demagnetization trajectories of those samples typically bypass the origin, indicating the presence of more than one component. Demagnetization trajectories hint at the fact that the higher-unblocking-temperature magnetization remaining during progressive demagnetization is south to southeast directed and thus that the samples are reversely magnetized. The polarity was not solely interpreted from demagnetization trajectories, as some specimens in this interval yield southeast magnetizations (with large MAD values but unambiguous polarity; Fig. 5e). Demagnetization trajectories of some specimens from sites tru25 and tru2 indicate characteristic magnetizations of (questionable) normal polarity. Other sites higher in the section provide excellent estimates of the ChRM of this unit, with well-defined, high-unblocking-temperature and shallow magnetizations that decay to the origin between 500 and 680 °C (Figs 5g and h). Typically, this is overprinted by a steep magnetization removed with AF (Fig. 5f). The large contribution of a cubic phase to the magnetic mineralogy of the Trujillo Formation is evident from IRM experiments (Fig. 7c). This observation, combined with the relatively low coercivities observed (Fig. 5g), suggests that prominent north-directed steep positive overprint at sites tru10 and bc11 is carried by magnetite or maghemite.

Redonda Formation

Samples from the Redonda Formation yield generally straightforward demagnetization results, although the remanence is generally multi-vectorial. The ChRM is in all cases north directed and shallow, unblocking between about 500 and 690 °C (Figs 6a and b). Two distinct magnetization components that are different from the recent dipole field are superimposed on the ChRM, and are only revealed during thermal demagnetization. Some specimens from sites red13 and red15 near the base of the formation are characterized by an ill-defined and small magnetization component, generally removed between 200 and 400 °C (Fig. 6a), which has south-southwest-directed declinations and shallow inclinations. It is unclear whether this magnetization reflects recording of a reverse polarity field soon after the high-unblocking-temperature magnetization was locked in, or whether it reflects partial overprinting at a much later time. The mean derived from all samples containing this magnetization is poorly defined and not statistically different from the ChRM. Specimens from sites 17 to 19, all within the uppermost 5 m of the Redonda Formation, are characterized by an intermediate unblocking temperature overprint (Fig. 6d), removed between 400 and 600 °C with (*in situ*) moderately steep negative inclinations and north-directed declination. Separation of this overprint from the ChRM is generally straightforward. One site collected in the Middle Jurassic (Callovian) Entrada Formation immediately overlying the Redonda Formation gives a high-unblocking-temperature (and high-coercivity) magnetization indistinguishable from the intermediate temperature overprint in the uppermost 5 m of the Redonda Formation (Fig. 6e). Because of their similarity to the ChRM of the Entrada Formation, we interpret intermediate-temperature magnetizations in the Redonda Formation as secondary, with an age identical to that of the Jurassic sandstones. High resistance to AF demagnetization suggest that the ChRM and the intermediate temperature overprint observed in samples of the Redonda Formation are carried by haematite.

ROCK MAGNETISM AND IDENTIFICATION OF MAGNETIC CARRIERS

Rock magnetic data and petrographic observations include IRM acquisition and demagnetization experiments (Fig. 7), hysteresis loops for selected specimens (Fig. 8), as well as observations under the petrographic microscope. Haematite is the dominant magnetic carrier of the characteristic magnetization, except for beds in the lower parts of the Trujillo Formation, which are dominated by magnetite (or maghemite). The contribution from magnetite (or maghemite) to the natural and high-field remanence, estimated by the relative intensity of the magnetization removed with alternating fields, is variable. Magnetite (or maghemite) is the likely carrier of the low-temperature and low-coercivity magnetization parallel to the recent field direction, because this magnetization is generally soft.

All of the IRM acquisition curves illustrated in Fig. 7 were obtained from medium- to fine-grained sandstones, with the exception of sample gc9b, which is a pebble conglomerate with clasts of siltstone and fine-grained sandstone. In the two fluvial-channel sandstone-dominated formations (Santa Rosa and Trujillo Formations) there is greater colouration, grain-size and compositional variation. IRM acquisition curves of the Santa Rosa and Trujillo samples are haematite dominated, magnetite dominated, or haematite–magnetite mixtures. In contrast, samples of the Anton Chico, Garita Creek and Redonda Formations (which are mudstone dominated) are relatively homogenous, and are dominated by haematite.

The shapes of normalized intensity decay plots during thermal demagnetization in haematite-dominated clastic rocks (redbeds) have generally been interpreted to reflect the relative contributions of coarse-grained specular haematite and fine-grained pigmentary haematite (Collinson 1974). If most contributions from soft magnetic phases are isolated (by normalizing the curves by the intensity after the 200 °C step), behaviour varies, but a majority of the samples are characterized by relatively narrow ranges of unblocking temperatures above 600 °C (Fig. 8a). This suggests that specular haematite is the most important form of haematite contributing to ChRM. Distributed unblocking temperatures in samples of the Redonda Formation suggest that relatively equal contributions from coarse specular and fine-grained haematite are more typical of these rocks.

Hysteresis loops on selected specimens from all formations exhibit high coercivities (~100 mT) and 'wasp-waisted' geometries (Fig. 8b). Hysteresis parameters Hcr/Hc and Mrs/Ms plotted in a Day, Fuller & Schmidt (1977) diagram form a tight group with low Hcr/Hc values between 2.5 and 4 and

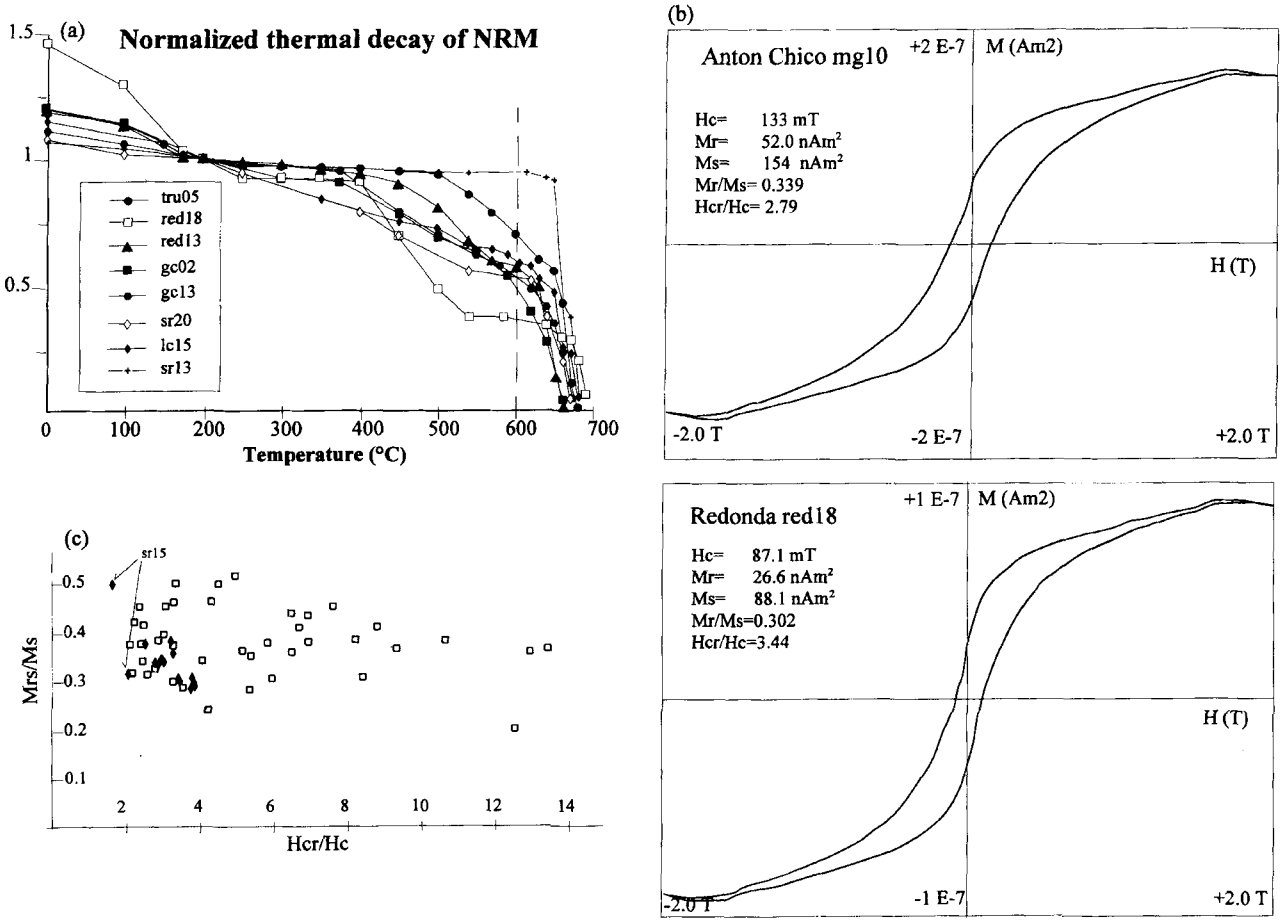

Figure 8. (a) Normalized (at 200 °C) decay of the NRM during thermal demagnetization of selected specimens. (b) Typical hysteresis loops for haematitic sandstone specimens of the Anton Chico Member of the Moenkopi Formation and the Redonda Formation Chinle Group. (c) Day *et al.* (1977) plot of hysteresis parameters of selected haematitic fine-grained sandstone specimens of the Anton Chico Member and Chinle Group (solid diamonds) compared with data for haematitic (red and pink) pelagic limestone (open squares; after Channell & McCabe 1994).

high Mrs/Ms values of about 0.3 (Fig. 8c). Two outliers are specimens from site sr15, whose demagnetization characteristics are different than those of all other sites. We compare these values with those from red and pink Tethyan pelagic limestone, whose magnetization is typically carried by haematite (Channell & McCabe 1994). Pelagic limestones (Fig. 8) are characterized by a large spread in Hcr/Hc values, with values as high as 35. The difference between the two populations suggests a fundamental difference between the characteristics of haematite in pelagic limestone and redbeds. Pelagic limestones are typically devoid of coarse-grained specular haematite and have lower and more distributed unblocking temperature spectra than redbeds.

INTERPRETATION

The North American APWP

Directions calculated for the ChRM (Fig. 9) are corrected for bedding attitude assuming a horizontal tilt axis (=bedding strike). Site and formation means with associated statistical parameters (Table 1) show that magnetizations isolated are for the most part well grouped. The relatively coarse-grained Santa Rosa and Trujillo Formations show moderate between-site dispersion, and for some sites relatively large within-site dispersion. Where normal and reverse polarity magnetizations were observed, reversal tests were applied after McFadden & McElhinny (1990). The angles between the mean normal and (inverted) reverse polarity directions (Table 1) are small (ranging between 2.7° and 11.5°). Of all subsets, only the Trujillo Formation failed the reversal test (the observed angle between normal and reverse directions is significant at the 5 per cent level). Positive reversal tests for the Anton Chico and Santa Rosa Formations are of category B (McFadden & McElhinny 1990) because critical angles are greater than 10°. For sites collected in the Anton Chico Formation, the estimated precision parameter, k, of the *in situ* distribution of site means is larger ($k=65.1$) than for the tilt corrected distribution ($k=45.1$). The decrease is not statistically significant; this result, rather than indicating a negative fold test, suggests that magnetization components may not be completely isolated or that the tilt correction does not incorporate the complete 'fold' geometry. The Anton Chico sites at La Cueva are of uniform reverse polarity and give shallow positive inclinations (average=3.5°), whereas at Montezuma Gap magnetizations are of dual polarity but the mean inclination is shallow negative (average=−9.2°). It is thus possible that directions at La Cueva are contaminated by a small secondary component of positive inclination. This would explain the decrease of the precision parameter, although we notice that demagnetization

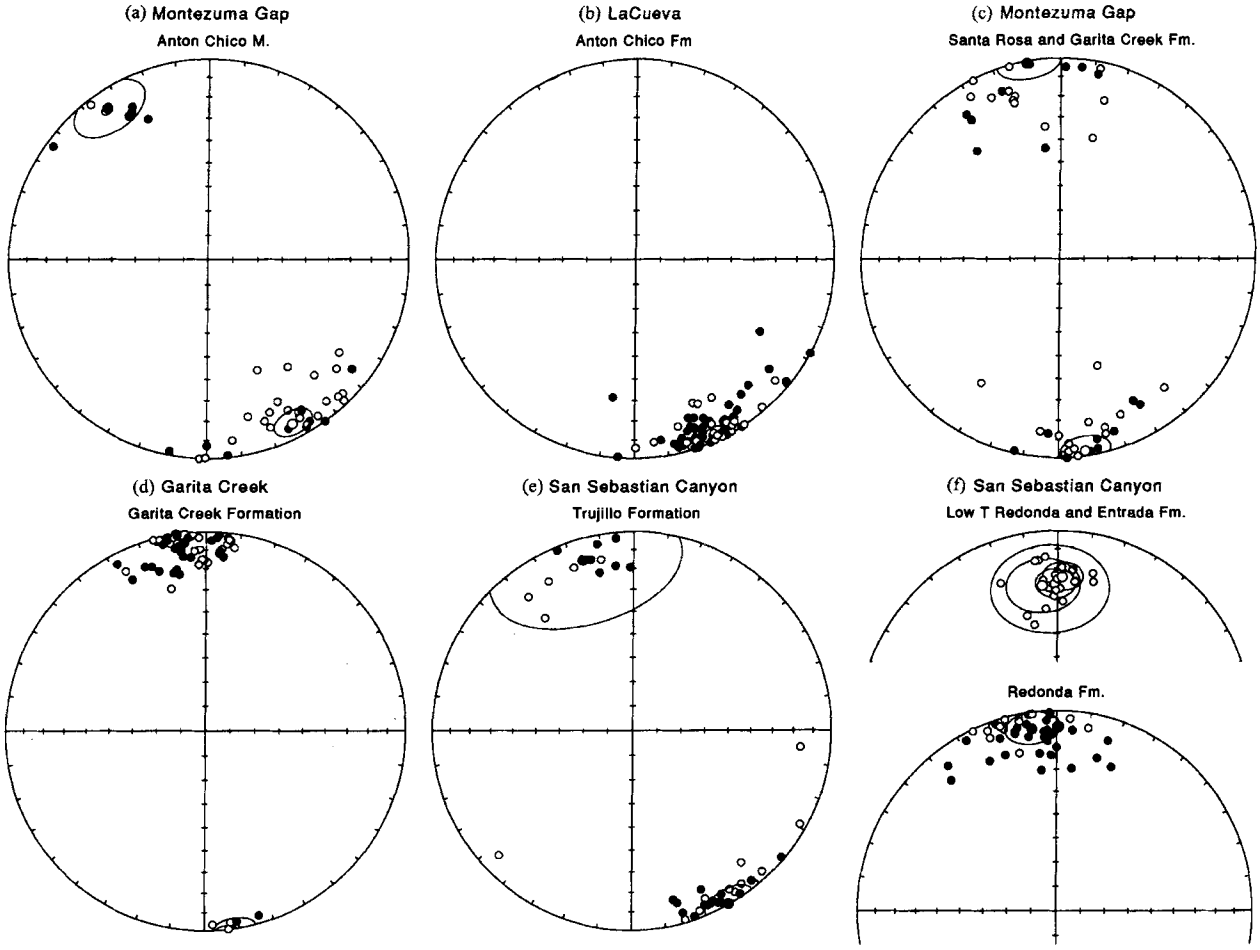

Figure 9. Equal-area projections of the (tilt-corrected) characteristic magnetizations isolated in samples of the Anton Chico Member (a and b), Santa Rosa Formation (c), Garita Creek Formation (d), Trujillo Formation (e), and Redonda Formation (f).

Table 1. Palaeomagnetic data and statistical parameters. Sangre de Cristo uplift and Tucumcari basin, eastern New Mexico. Dis-Iis (Dtc-Itc) = Site mean declination and inclination in geographic (tilt corrected) coordinates. N/n = number of samples (sites) demagnetized/used for site mean calculation. * Indicates sites excluded from the final calculation according to the selection criteria n < 3, k < 15, and α95 > 20. Mean poles are the Fisherian mean of site VGPs. γ, γ* = reversal test parameters after McFadden & McElhinny (1990).

Site	D(°) is	I(°) is	D(°) tc	I(°) tc	N\n	k	α95(°)	VGP °N	VGP °E
Bernal (Late Permian)									
mg2	164.2	38.5	136.4	-15.5	5\5	210.0	5.3	41.6	140.7
mg3	169.0	30.3	144.1	-10.4	5\5	43.0	11.8	45.2	130.8
Mean	**166.7**	**34.4**	**140.3**	**-13.0**	***10 samples***			**43.5**	**135.8**
Anton Chico Fm. -Montezuma Gap (Middle Triassic)									
mg4	161.5	24.5	324.4	7.2	5\5 n-r	24.5	15.8	44.2	128.8
mg5	347.1	-27.0	331.4	13.3	5\5	34.0	13.5	51.0	123.8
mg6	158.0	24.3	156.2	-23.0	5\5	48.0	13.4	58.1	123.0
mg7	167.8	28.0	151.8	-14.5	5\5	72.0	9.1	51.8	124.0
mg8	169.3	21.0	154.1	-8.4	7\7	12.0	17.9	50.6	118.1
mg10	163.1	28.5	138.7	-5.3	5\5	28.5	14.6	39.6	133.6
mg11	170.0	27.6	143.5	-2.7	5\5	52.0	10.7	41.9	127.7
mg12	172.5	-8.2	179.1	2.1	4\4	241.0	5.9	55.5	76.3
normal			326.4	9.7	7	25.0	12.3		γ=5.9
reverse			152.3	-8.6	33	16.0	6.4		γ*=14.6
Mean	**166.2**	**21.8**	**152.3**	**-9.2**	**8\8**	**31.6**	**10.0**	**50.2**	**121.0**
Anton Chico Fm. -La Cueva (Middle Triassic)									
lc01*	154.5	23.6	145.9	3.0	4\4	13.7	25.8	40.9	122.6
lc02	159.8	23.8	149.7	6.1	3\3	41.6	19.4	41.8	117.3
lc03*	151.6	16.1	148.0	-4.6	3\3	11.8	37.6	45.2	123.5
lc04*	174.5	9.3	169.8	3.6	5\5	6.3	33.0	51.1	91.1
lc05	156.4	23.9	147.2	4.3	5\5	301.4	4.4	41.2	120.7
lc06	167.1	14.2	161.1	2.8	5\5	273.6	4.6	48.7	104.2
lc07	161.8	24.6	150.7	7.8	5\5	61.2	9.9	41.7	115.6
lc08	162.8	20.9	153.7	5.5	5\5	250.2	4.8	44.2	112.9
lc09	172.0	19.4	161.4	9.8	5\5	427.3	3.7	45.6	101.8
lc10	163.0	20.9	153.9	5.6	4\4	147.2	7.6	44.3	112.6
lc11	165.5	15.7	158.9	3.0	3\3	81.3	13.8	47.7	107.1
lc12*	156.3	23.1	147.6	3.6	5\5	12.4	22.6	41.7	120.6
lc13	160.1	11.4	157.4	-3.6	5\5	26.6	15.1	50.0	111.4
lc14	166.1	11.5	162.0	0.1	5\5	133.6	6.6	50.3	103.7
lc15	155.2	28.0	143.8	7.0	5\5	22.0	16.7	38.1	123.2
lc16	170.2	13.4	163.9	4.1	5\5	375.8	4.0	49.2	99.8
lc17	153.9	11.5	152.5	-7.1	5\5	30.4	14.1	48.9	119.3
Mean	**162.7**	**18.5**	**155.1**	**3.5**	**13\17**	**108.5**	**4.0**	**45.8**	**111.9**
Santa Rosa Fm.-Montezuma-Gap (late Carnian)									
sr13	1.0	-10.9	343.7	-5.1	5\3	23.8	25.8	48.9	100.0
sr14	334.5	-24.2	333.1	24.5	5\5	23.2	16.1	56.8	128.3
sr16*	179.8	-2.6	177.3	5.0	5\1			51.9	79.1
sr17*	352.7	6.5	358.3	-1.7	5\3	11.0	39.1	53.6	77.6
sr18*	154.1	-0.5	176.0	-18.1	5\5	9.0	27.0	63.5	83.6
sr19	164.3	0.1	171.6	-5.5	4\4	75.5	10.6	56.3	90.0
sr20	168.6	-1.9	172.2	-0.8	4\4	62.0	11.7	54.1	88.1
sr21*	169.5	-7.9	177.7	1.8	5\5	8.5	27.8	53.5	78.6
sr22	172.7	5.1	164.3	1.1	4\4	18.5	21.9	51.0	100.2
Garita Creek Fm. - Montezuma Gap (late Carnian)									
gc23	352.7	6.8	355.7	-4.6	5\5	20.0	17.5	51.9	81.7
gc24	14.7	8.1	350.9	-25.9	5\5	29.0	14.5	40.0	86.3
normal			348.4	-2.5	21	10.2	10.5		γ=4.0
reverse			351.4	-5.1	23	15.6	7.9		γ*=12.7
Mean	**352.8**	**-3.4**	**347.5**	**-0.9**	**7\12**	**23.8**	**12.6**	**52.1**	**95.5**

Site	D(°) is	I(°) is	D(°) tc	I(°) tc	N\n	k	α95(°)	VGP °N	VGP °E
Garita Creek Fm. - Garita Creek (late Carnian)									
gc01	353.9	-8.7			6\6	55.6	9.1	49.9	85.1
gc02	356.9	-10.9			5\5	143.0	6.4	49.1	80.3
gc03-04	360.0	-11.3			8\8	237.6	3.6	49.0	75.6
gc05	351.1	-12.1			5\5	52.4	10.7	47.8	88.8
gc06*	357.9	6.6			5\5	14.2	20.6	58.0	79.6
gc07	5.2	1.3			5\5	266.9	4.7	55.0	66.5
gc09*	3.0	5.9			4\4	12.2	27.5	57.5	70.0
gc10	350.9	1.1			5\5	19.0	18.0	54.2	91.3
gc11	355.8	12.0			5\5	36.7	12.8	60.5	84.1
gc12*	354.7	12.6			4\6	4.9	46.6	60.7	86.4
gc13	171.4	0.1			5\5	156.5	6.1	53.8	90.2
gc14	352.6	6.8			4\4	42.3	14.3	57.4	89.4
gc15	349.9	-0.8			6\6	152.8	5.4	53.1	92.6
gc16	342.5	12.0			6\6	64.1	8.4	56.6	108.5
gc17	351.8	7.5			4\4	219.6	6.1	57.6	91.0
normal	353.9	-1.0			59	32.5	3.3		γ=2.7
reverse	171.4	0.1			5	156.5	6.1		γ*=6.6
Mean	**353.5**	**-0.3**			**12\17**	**59.9**	**5.7**	**54.1**	**86.7**
Trujillo Formation-Montezuma Gap (early Norian)									
tru25*	336.4	14.2	335.6	-15.1	7\3	8.8	44.3	41.0	107.6
tru26*	156.4	35.3	146.4	3.5	6\2			44.0	125.0
tru27-28	334.3	-19.5	342.3	29.5	10\3	26.8	24.3	64.7	117.9
Trujillo Formation-San Sebastian Canyon (early Norian)									
tru2*	340.6	-20.9	337.6	8.8	7\2			52.6	113.4
tru3	166.8	35.9	141.7	-12.3	6\3	63.2	15.6	44.3	134.1
tru4	177.4	10.8	157.2	6.9	5\3	107.1	12.0	45.4	108.2
tru5	172.0	15.7	153.1	1.0	5\5	53.1	10.6	46.0	115.4
tru6	170.8	12.7	156.2	0.2	4\4	94.3	9.5	47.9	111.8
tru7	171.7	15.8	162.0	-7.2	5\5	45.5	11.5	54.0	106.4
tru9	172.6	22.5	164.2	-14.9	4\4	113.2	8.7	58.6	105.9
tru10	14.3	-19.7	344.7	-5.5	4\4	19.3	17.8	49.2	98.5
Bull Canyon Formation-San Sebastian Canyon (early Norian)									
bc11	348.3	-13.1	354.3	18.5	4\4	33.6	16.1	63.3	89.5
normal			344.8	2.5	16	16.9	9.2		γ=11.8
reverse			153.4	0.6	26	52.4	4.0		γ*=9.9
Mean			**339.4**	**7.7**	**9\14**	**29.1**	**9.7**	**53.3**	**110.6**
Redonda Formation-San Sebastian Canyon (late Norian)									
red12	347.5	-6.5	356.3	14.0	4\4	134.8	7.9	61.2	82.4
red13	355.3	-10.8	351.0	7.0	6\6	62.1	8.1	56.8	91.3
red14	355.7	0.8	2.5	5.1	5\5	59.7	10.0	56.8	70.2
red15	351.6	-5.1	357.2	10.0	5\5	124.6	6.9	59.3	80.2
red16	355.6	-2.4	359.4	5.7	5\5	35.0	13.1	57.2	75.8
red17	333.6	-0.2	5.3	27.1	4\4	50.1	13.1	**68.2**	60.8
red18	11.1	2.8	2.3	-8.8	7\7	30.8	11.1	49.9	71.2
red19	9.0	-11.9	358.9	3.1	5\5	58.4	10.1	55.9	76.7
Mean			**359.1**	**7.9**	**8\8**	**54.7**	**7.6**	**58.5**	**76.5**
Redonda Formation-San Sebastian Canyon (low Temperature)									
red17	354.4	-27.8	344.8	18.8	5\5	36.1	12.9	60.5	106.4
red18	2.1	-23.8	348.7	11.8	6\7	96.5	6.9	58.5	96.7
red19	359.3	-27.3	345.3	14.5	5\5	122.5	6.9	58.7	103.7
Entrada Formation (lower Middle Jurassic)									
ent20	357.1	-28.8	343.7	16.7	4\4	20.2	21.0	59.1	107.4
Mean	**358.3**	**-27.0**	**345.6**	**15.4**	**4\4**	497.4	4.1	**59.3**	**103.5**

diagrams of Anton Chico samples show nearly linear trajectories to the origin above 630 °C (Fig. 4a). For late Carnian and early Norian sites the precision parameter remains basically unchanged after tilt correction.

Palaeomagnetic poles were calculated from site virtual geomagnetic poles (VGPs) for the Middle Triassic, late Carnian–early Norian, and late Norian. Sites with poorly defined means ($k < 15$; $n < 3$; and $\alpha 95 > 20°$) were excluded. A total of 11 sites were excluded from mean pole calculations using this criterion. Sites mg1, sr15 and tru1 did not give usable results; sites gc03-04 and tru27-28 were collected from the same layers and were combined in the final calculations.

The mean Middle Triassic, mid–Late Triassic, and late Late Triassic palaeomagnetic poles from the Sangre de Cristo Mountains (Table 2, Fig. 10) are statistically distinct from one another, and they reproduce the main features of the North American Triassic APWP. The poles are spread along an approximately east–west-trending arc of about 25° length. Each of the VGP distributions is typically elliptical and elongate along the trend of the APWP (Fig. 10, Table 2). To assess the uncertainties introduced by the tectonic correction, data from steeply dipping strata were compared with results from similar age but gently dipping or flat-lying strata. If the tilt axis is not horizontal, a systematic bias will affect the palaeomagnetic declinations. For the geometry of the tilt axis and directions of magnetization at Montezuma Gap and San Sebastian Canyon, a tilt axis inclined by about 5° will affect the declination by about the same amount.

A comparison of palaeomagnetic directions from steeply dipping strata and horizontal or gently dipping strata (below) suggests that a small, though appreciable, apparent tectonic rotation of less than 5° in an anticlockwise sense may affect declinations. The small number of samples collected from Upper Permian strata do not allow for a tectonic interpret-

Table 2. Summary of Triassic palaeomagnetic poles for the Sangre de Cristo Mountains and the craton interior (Texas and New Mexico) and North America reference poles (Triassic through Early Jurassic) including data from the Colorado plateau corrected as explained in the text. N (n) is the number of palaeomagnetic sites (samples) used in the pole calculation. K and α95 are the parameters of the Fisher distribution; k1, k2 α12, and α13 are the precision parameters and the semiaxes of the ellipse that approximates the 95 per cent confidence region of a Bingham distribution. The trend of the major semiaxes given as the oval azimuth (ov.az.). Poles in parentheses are before correction for the 4° plunge of the tilt axis. Average poles N. America # do not include poles from this study or the Colorado Plateau; these poles were used to examine the possibility of apparent tectonic rotations in the Sangre de Cristo poles. ## Pole recalculated from data in Reeve & Helsley (1972). (1) Grubbs & Van der Voo (1976), Van der Voo & Grubbs (1977; 2 poles); Shive *et al.* (1984); Herrera-Bervero & Helsley (1983); Baag & Helsley (1974); Helsley & Steiner (1974); Helsley (1969); McMahon & Strangway (1968); Purucker *et al.* (1980); Molina-Garza *et al.* (1991); This study.
(2) Fang & Van der Voo (1988; 2 poles); Van der Voo & Grubbs (1977); Witte & Kent (1989); Symons *et al.* (1989); Molina-Garza *et al.* (1991); Molina-Garza *et al.* (1995); This study.
(3) Bazard & Butler (1991; 2 poles); Larrochelle & Currie (1967); Witte *et al.* (1991).
(4) Reeve and Helsley (1972); Kent & Witte (1993); Molina-Garza *et al.* (1995); This study.
(5) Ekstrand & Butler (1989); Molina-Garza *et al.* (1995); Kodama *et al.* (1994a,b); Smith (1987).

	Symbol	N	k1	k2	α13	α12		Pole		Reference
		[n]		K		A95	ov.az.	°N	°E	
Middle Triassic (~235 Ma)										
Anton Chico (ClinesCorner)	ac0	*[22]*		29.7		5.8		43.9	120.8	Steiner and Lucas 1992
Anton Chico (Montez. Gap)	ac1	8	-128.8	-13.7	3.2	9.9	120.0	51.8 (50.2)	116.7 (121.0)	
Anton Chico (La Cueva)	ac2	13	-339.0	-46.6	1.5	4.1	123.3	45.8	111.8	
Combined	ac	**21**	**-88.8**	**-24.0**	**2.3**	**4.5**	**120.2**	**48.0**	**113.5**	
N. America#		*6*		*191.7*		*4.9*		*46.7*	*113.8*	Molina-Garza et al. 1995
Carnian-Early Norian (~225 Ma)										
S. Rosa and Garita (Montez.Gap)	sr	7	-88.7	-21.0	4.1	8.4	59.5	53.1 (52.1)	88.8 (95.4)	
Trujillo Bull-Canyon (Sebas.can.)	tr	9	-51.8	-23.6	4.7	7.0	137.5	54.9 (53.2)	104.1 (110.5)	
Garita Creek (Garita Creek)	gc	12	-119.8	-50.3	2.6	4.1	70.7	54.0	86.7	
Combined	sr-tr	16	-40.7	-21.1	4.0	5.6	84.9	54.4 (53.0)	97.3 (103.8)	
Combined	sr-gc-tr	**28**	**-56.5**	**-24.4**	**2.5**	**3.9**	**81.4**	**54.3**	**92.6**	
Dockum Group, W. Texas	dg	12		44.2		6.6		56.4	96.3	Molina-Garza et al. 1995
Bull Canyon (Upper Shale)	bc	15		60.0		5.0		57.4	87.8	Bazard and Butler 1991
N.America#		6		270.7		4.1		50.9	97.1	Molina-Garza et al. 1995
Late Norian-Rhaetian (~210 Ma)										
Redonda (Sebas.can.)	rd1	**8**	**-104.9**	**-64.9**	**3.5**	**4.4**	**156.6**	**58.3 (58.5)**	**68.9 (76.5)**	
Redonda (Tucumcari basin)	rd0	2		22.0		6.0		61.4	72.4	Bazard and Butler 1991##
Tecovas B (reverse), W. Texas		7		204.2		4.2		59.3	77.8	Molina-Garza et al. 1995
Tecovas B (normal), W. Texas		7		62.4		7.6		59.0	53.8	Molina-Garza et al. 1995
N.America reference poles.										
(240 Ma)		*12*		*195.6*		*3.1*		*51.6*	*110.1*	1
(228 Ma)		*8*		*190.1*		*4.0*		*53.0*	*96.9*	2
(220 Ma)		*4*		*290.1*		*5.4*		*57.4*	*84.6*	3
(210 Ma)		*4*		*313.1*		*1.6*		*59.7*	*70.3*	4
(200 Ma)		*4*		*486.1*		*4.2*		*59.2*	*60.5*	5
lower Middle Jurassic (175 Ma)										
	ent	4						60.7 (59.3)	96.1 (103.5)	

ation, although we note that the declination of the mean direction (dec = 140.3°, inc = −13°) is to the east of the expected value (dec = 152°, using the Late Permian cratonic reference pole of Van der Voo 1990) and results in a significant declination anomaly (12.2° ± 8°).

The Middle Triassic palaeomagnetic pole at Montezuma Gap (ac1) is statistically indistinguishable from a recently published Mid-Triassic pole from flat-lying Anton Chico strata near Clines Corner, about 60 km south of Las Vegas (ac0, Table 2, at 43.9°N 120.8°E; Steiner & Lucas 1992). Pole ac0, however, barely satisfies modern reliability criteria because it was derived from the mean of only 22 samples, all of normal polarity. Pole ac1 falls east of pole ac2 obtained from gently dipping strata at La Cueva (45.8°N 111.8°E). The difference between ac2 and ac1 declinations is 2.8° (± 7.8°). Pole ac1 also falls east of the mean Middle–Early Triassic cratonic reference pole (46.7°N 113.8°E) calculated combining pole ac0 with five older poles obtained from the Lower Triassic Chugwater Formation and related strata in Wyoming cited in Van der Voo (1990). The observed ac1 declination is 2.3° (± 8°) less than expected from the cratonic reference pole. The difference is not statistically significant at the 95 per cent level of confidence.

The late Carnian–early Norian pole of steeply dipping strata (sr–tr) includes sites collected in the Santa Rosa (5), Garita Creek (2), Trujillo (8), and Bull Canyon (1) Formations. The mean declination for the (younger) Trujillo and Bull Canyon Formations is about 8° east of the mean of the Santa Rosa and Garita Creek Formations. That is opposite to the general trend of the APWP. It is difficult to assess the significance of this observation, because the means have relatively large uncertainties (α95 > 10°). The means are not statistically different (at the 95 per cent confidence level) and both data sets were combined for the next level of analysis: a comparison between the mean direction of steeply dipping strata (sr–tr) and horizontal strata (gc: Garita Creek locality). This comparison results in a declination anomaly of 10° (± 6°). Using another cratonic pole (the Dockum Group in west Texas, at 56°N 96°E; Molina-Garza, Geissman & Van der Voo 1995), the discrepancy is still large and statistically significant (5.3° ± 4.2°).

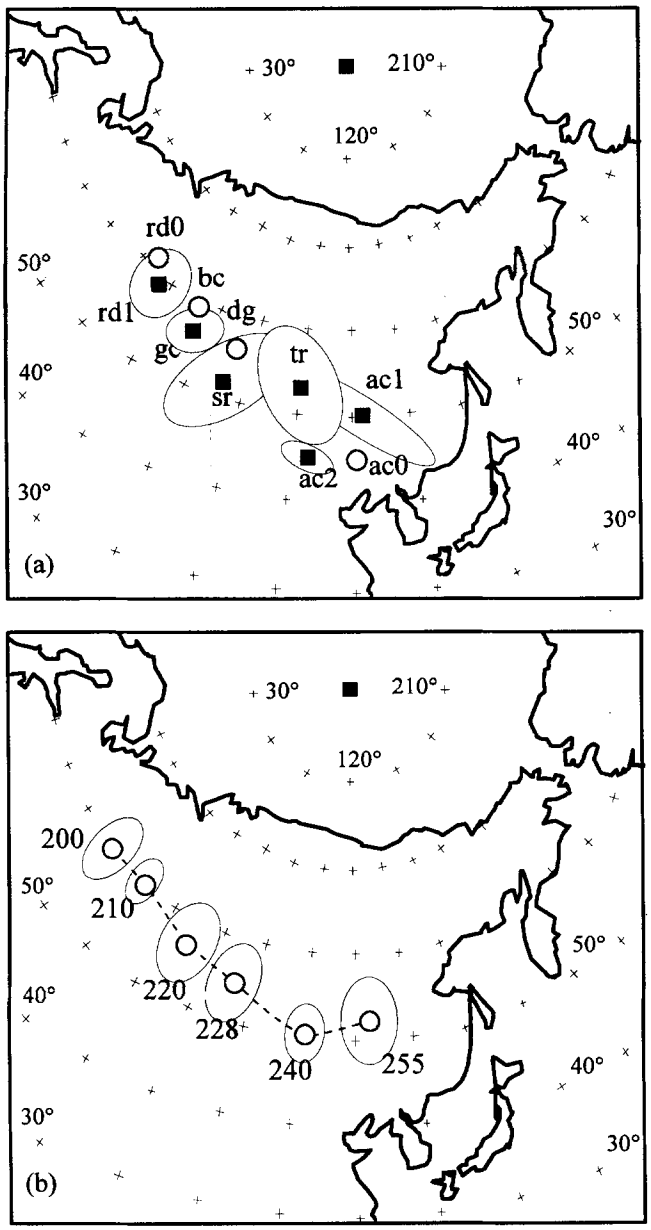

Figure 10. (a) Mean palaeomagnetic poles (based on VGPs) obtained in this study with 95 per cent confidence ellipses (calculated using Bingham statistics). Symbols as in Table 2. (b) North American Triassic apparent polar wander path. Mean poles (circles with confidence regions = A95) calculated from data in Molina-Garza *et al.* (1995) and results from this study. The Late Triassic data have been subdivided into three subsets. The mean poles include palaeomagnetic data from the Colorado plateau, which have been corrected by rotating the poles 4° about a rotation pole at 36°N 105°E. The mean Triassic poles are listed in Table 2.

Finally, for the Redonda Formation, comparison with the expected direction using the pole rd0 recalculated by Bazard & Butler (1991) from data in Reeve & Helsley (1972) and obtained from flat-lying Redonda Formation strata in the Tucumcari basin gives a declination anomaly of 2.2°(±6°). The difference is again small and not statistically significant. In summary, all four means have small declination anomalies, all of which are in the same anticlockwise sense. The anomalies are only significant for the Late Permian mean and the late Carnian–early Norian mean.

Because of the general consistency of the declination anomalies, it is possible that a small, yet appreciable, bias exists in the data from sections at Montezuma Gap and San Sebastian Canyon. The apparent tectonic rotation is no more than about 4°, the average of the declination anomalies observed between the Triassic poles compared. This apparent rotation is equivalent to a tilt axis plunging gently to the south. This is consistent with the abrupt termination of the mountain range south of Las Vegas. Incorporating a correction for the gentle plunge of the tilt axis and combining all Anton Chico sites, we obtained a mean Anisian pole (ac, ~240 Ma) at 46.7°N 113.4°E ($N=21$ sites) that is in excellent agreement with the reference APWP, and supersedes pole ac0 of Steiner & Lucas (1992). Similarly, a late Carnian–early Norian pole (sr–gc–tr, ~225 Ma) falls at 54.3°N 92.6°E ($N=28$ sites), the late Norian–Rhaetian (~208 Ma) Redonda Formation gives a pole at 58.3°N 68.9°E ($N=8$ sites). The Redonda pole is based on a smaller number of sites and at all sites ChRMs are of normal polarity. Based, however, on its similarity to a previous pole determination for this unit and the quality of the demagnetization data, there is little doubt of the reliability of this result.

The Triassic segment of the North American APWP is the subject of recent controversy (Bazard & Butler 1991; Molina-Garza *et al.* 1991; Kent & Witte 1993; Molina-Garza *et al.* 1995). We believe that the above analysis of our new data shows that, despite the large amplitude of the tectonic correction and the location of the sites within the Laramide deformation belt, objections to the use of palaeomagnetic poles from the Sangre de Cristo uplift to further define the cratonic APWP are unfounded. Three Triassic palaeomagnetic poles from this study are in good agreement and define a consistent age progression from Middle to latest Late Triassic. They further support previously published results from western and southwestern North America and suggest a relatively large magnitude (~25° of arc) and a relatively rapid rate of APW.

A refined Early Mesozoic APWP for stable North America (Fig. 10b) includes our new results. Poles averaged include results from the Colorado plateau, which have been corrected by rotating the poles 4° about a pole at 36°N 105°W. Our new results for the Anton Chico Member suggest that rotation of the plateau is smaller than previously inferred by comparison of Early–Middle Triassic poles (Steiner 1986). The angular distance between the Anton Chico pole of this study and Moenkopi poles on the plateau is 11.9°±4.8° (95 per cent confidence). There is a large difference in inclination between the expected and observed directions of Moenkopi strata. It is thus possible that Moenkopi poles determined by previous workers in Colorado and Arizona are contaminated by younger magnetizations. When compared with recently published results for the age-equivalent Rock Point Formation (Church Rock Member; Kent & Witte 1993), results for the Redonda are inconsistent with a large rotation of the plateau.

Triassic poles from North America are divided into four groups, including Early and Middle Triassic poles (~240 Ma), Carnian–early Norian poles (~228 Ma), early and middle Norian poles (~220 Ma), and late Norian–Rhaetian poles (~210 Ma). Absolute ages were inferred from stratigraphic ages using the time-scale of Harland *et al.* (1990). Poles (Table 2) were selected from compilations by Van der Voo (1990), and include poles of Q factor greater than or equal to

four. We excluded poles superseded by more recent investigations, such as the Church Rock pole of Reeve (1975) and the Newark pole of McIntosh, Hargraves & West (1985). The location of the Early Jurassic cusp (~200 Ma) at about 60°N 60°E is from Molina-Garza *et al.* (1995). The Hettangian pole for the Newark extrusive zone and the poles published by Van Fossen, Flynn & Forsythe (1986) were excluded because of questions raised by Molina-Garza *et al.* (1995) and Kodama *et al.* (1994a) regarding their reliability; in particular, structural complications associated with their proximity to the border fault of the Newark basin and the observation of a thermal overprint of presumed Hettangian age in the Culpeper basin by Kodama *et al.* (1994b), which is significantly displaced from the Hettangian pole of Witte & Kent (1990).

A preliminary palaeopole derived from one site in the Middle Jurassic Entrada Formation (Callovian?, ~175 Ma) and secondary magnetizations in the Redonda Formation falls at 59.2°N 103.5°E (Fig. 10b). Based on demagnetization behaviour, the intermediate unblocking temperature magnetization isolated in the Redonda Formation is not a composite magnetization resulting from simultaneous removal of the present-day field and a Late Triassic field (such a composite would result in a shallow to intermediate positive inclination vector). Because we report four VGPs, we can only offer a tentative interpretation that magnetizations in the Entrada Formation are near primary, and low-temperature secondary magnetizations in the uppermost beds of the Redonda were acquired during remanence acquisition in the overlying Entrada beds, possibly by remobilization of fine-grained haematite due to weathering.

Magnetostratigraphic correlation of Triassic strata

Magnetostratigraphic correlation of the Moenkopi Formation data (Fig. 11) with the record of marine rocks (after Steiner *et al.* 1989; Ogg & Steiner 1991; Muttoni & Kent 1994; Muttoni *et al.* 1994) suggests that Moenkopi strata represent parts of the Dienerian, Smithian, Spathian and Anisian stages. Direct correlation with the marine biochronology is supported by the late Smithian index fossil *Meekoceras* in the Sinbad Limestone and the well-accepted Spathian age of *Tirolites* in the Virgin Limestone. Previous attempts to correlate the magnetostratigraphy of the Moenkopi Formation (e.g. Shive *et al.* 1984) encountered difficulties explaining the predominantly normal polarity of the Moenkopi sequences studied in Arizona (Elston & Purucker 1979) and the predominantly reverse polarity of sequences sampled in Colorado and Utah (Helsely & Steiner 1974; Lienert & Helsely 1980). An intraformational unconformity at the top of the Ali Baba Member of the Moenkopi Formation can explain the difference between

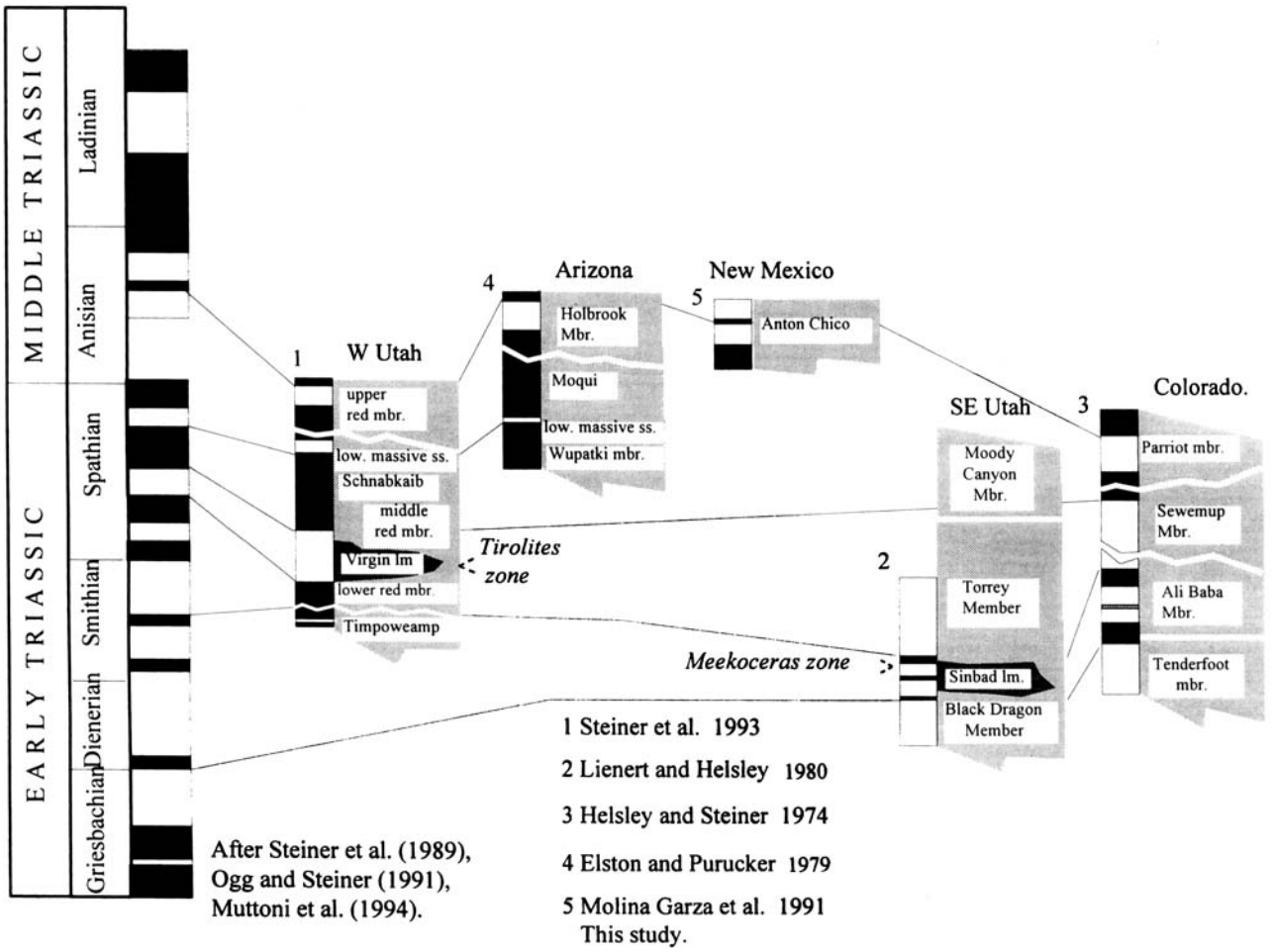

Figure 11. Proposed correlation of the magnetic polarity sequence of the Moenkopi Formation with that obtained from Early and Middle Triassic marine strata.

the sections studied in Colorado and Arizona (Fig. 11). Our correlation suggests that the Sewemup Member in Colorado is correlative with the Virgin Limestone and the middle Red Member in western Utah and that the Wupatki Member in Arizona is younger than the Sewemup Member. This correlation is supported by new lithostratigraphic data (Lucas 1995) that indicate the Sinbad Limestone intertongues eastwards with the Ali Baba Member in the Canyonlands area, eastern Utah (Lucas 1995), not with the Sewemup Member as previously stated (Shoemaker & Newman 1959). A second unconformity separates Holbrook Member strata from the underlying Moqui Member. Litho- and biostratigraphic correlation of the Anton Chico and Holbrook Members is well established (Morales 1987; Lucas & Morales 1985). Correlation of Holbrook strata with the Parriot Member in Colorado and the upper Red Member in western Utah is less certain.

The Late Triassic magnetic polarity sequence is based on the work of Gallet *et al.* (1992, 1993, 1994) and Kent *et al.* (1995). Notice, however, that different chronologies are involved in those studies. Gallet *et al.* calibrated Tethyan pelagic sequences using the assumption of equal-biozone duration, whereas Kent *et al.* calibrated the Newark lacustrine sequence with an interpreted astronomical cyclicity and placed the Triassic–Jurassic boundary at 202 Ma. The presence of several hiatuses in the Chinle section and the facts that Chinle group sections are typically thin and are dominated by mudstones make it obviously difficult to make independent correlations with either the Newark or the Tethyan sequences. Magnetostratigraphic correlation in the Chinle Group and related strata (Fig. 12) is, however, consistent with biostratigraphic data, which suggest that the base of the Chinle Group (Shinarump and Agua Zarca Formations and Tecolotito

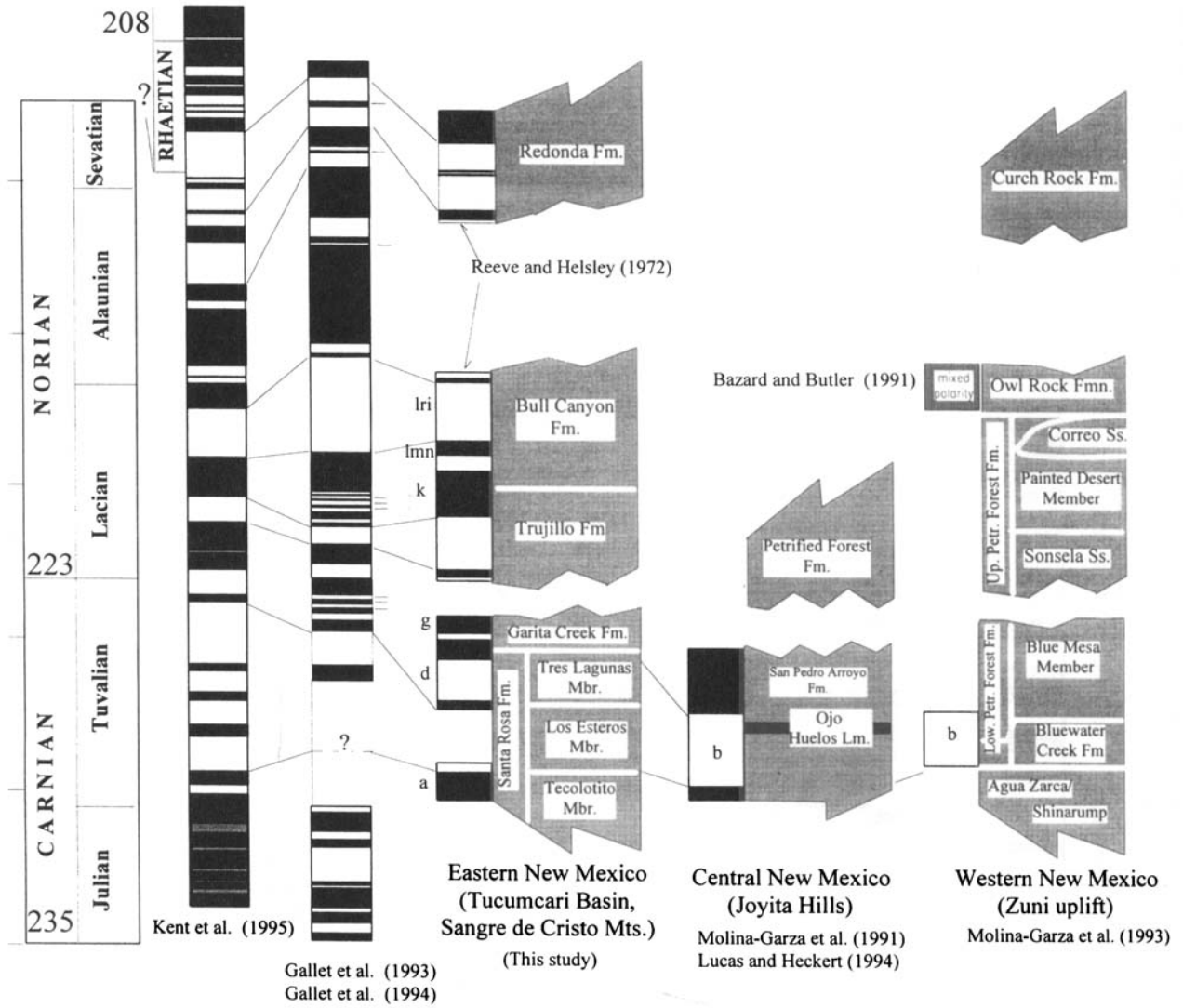

Figure 12. Proposed correlation of the magnetic polarity sequence of the Chinle Group with that obtained from Late Triassic marine strata (Gallet *et al.* 1993, 1994) and non-marine strata of the Newark rift basin (Kent *et al.* 1995). Note that the magnetic polarity sequence of Chinle strata in central New Mexico has been revised (Agua Zarca Member and San Pedro Arroyo Formation). The Agua Zarca Member (Tejon section, in Molina-Garza *et al.* 1991) underlies San Pedro Arroyo strata, therefore the normal polarity zone in the San Pedro Arroyo (Sevilleta section of Molina-Garza *et al.* 1991) does not correlate with the normal polarity zone observed in the Agua Zarca. The lower part of the San Pedro Arroyo Formation correlates in part with the Bluewater Creek Formation in western New Mexico, where it is of reverse polarity. Polarity intervals in the lower Chinle Group are labeled a to k as in Fig. 3. In the upper Chinle Group labels lmn (lower most normal) and lri (long reverse interval) follow Reeve & Helsley (1972). Time-scale after Harland *et al.* (1990).

Member of the Santa Rosa Formation) are lower Tuvalian (lower upper Carnian). The time represented by strata of Otischalkian faunachron (early Tuvalian) is difficult to assess. These strata are generally thin and apparently of predominantly normal polarity. Pelagic sections sampled by Gallet *et al.* (1992, 1993, 1994) do not contain early Tuvalian data, and temporal resolution in age-equivalent strata in the Newark basin (Stockton Formation) is relatively poor (Kent *et al.* 1995). Nonetheless, biostratigraphic data (Huber, Lucas & Hunt 1993) suggest that the lower strata of the Chinle Formation correlate in part with the Stockton Formation of the Newark Supergroup. The lower beds of the Santa Rosa Formation are *Paleorhinus* bearing strata of the Otischalkian faunachron (Lucas 1993; Lucas & Hunt 1993). *Paleorhinus* occurs in the lower Tuvalian Opponitzcher Schichten strata of the Austrian Alps (Hunt & Lucas 1991) and the Pekin Formation of the Chatham Group in North Carolina (Huber *et al.* 1993). In Fig. 12 we suggest that predominantly normal polarity intervals at the base of the Stockton and Chinle sections are correlative, at least in part.

Comparison of the Chinle composite with the Tethyan polarity sequence suggests that very short polarity intervals of duration of about 10^4 yr near the Carnian–Norian boundary and in the lower Norian (Lacian 1) are not recorded by Chinle strata (Fig. 12). These short events were also not observed in the Carnian–Norian Newark record (the b+, c− and d+ zones of Kent *et al.* 1995). The reliability of short intervals in the pelagic sequence is questionable because some are defined by a single sample. The Chinle sequence, however, reproduces some of the main features of the Late Triassic marine and non-marine records. We correlate long reversed polarity intervals in the Bluewater Creek Formation, Lower San Pedro Arroyo Formation, and Tres Lagunas Member of the Santa Rosa Formation (intervals b and d; Fig. 3) with the dominantly reversed intervals in the Lockatong Formation and the late Tuvalian pelagic record.

The comparison of polarity sequences suggests that most of the middle Norian (the Alaunian of the pelagic sequence, and middle Norian zones f+ to h+ in the Newark sequence) is not represented by Chinle strata in eastern New Mexico. The presence of a profound hiatus had been previously inferred based on the more advanced characteristics of phytosaurs in the Redonda Formation and more abundant dinosaur fossils. Lucas (1991, 1993) suggested the base of the Redonda Formation is an unconformity (Tr-5 unconformity) of basin-wide extent in the Chinle Group depositional basin. Hunt (1991) first suggested, followed by Lucas (1993) and Lucas & Hunt (1993), that vertebrate fossils from the Redonda Formation indicate a possible Rhaetian age.

Our sampling in the Bull Canyon and Redonda Formation is much less detailed than that of Reeve & Helsley (1972). The magnetostratigraphy is consistent with the polarity sequence of Reeve & Helsley (1972). The lowermost beds and the uppermost beds of the Redonda at Luciana Mesa and Redonda Mesa in eastern New Mexico are of normal polarity. The lack of exposure did not allow us to sample a 25 m interval of the Redonda at San Sebastian Canyon. Unfortunately, from the section published by those authors, it is unclear whether or not a complete Bull Canyon (upper shale) sequence was collected. Thus, the normal polarity observed at the top of the Trujillo Formation and in one site in the Bull Canyon Formation in the San Sebastian section (our interval k; Figs 3 and 12) may or may not be the 'lowermost normal interval' of Reeve & Helsley (1972, p. 3797). Based on the general thickness of the Bull Canyon Formation we believe that a complete Bull Canyon section was not sampled by those authors and that the lowermost reverse interval of Reeve & Helsley (1972) overlies our interval k. We thus correlate most of the Bull Canyon's 'long reverse interval' with the upper Lacian (Lacian 3, KTB-) reversed interval in the pelagic sequence and the reversed interval containing the Perkaise Member of the Passaic Formation (e−). This is consistent with sequence stratigraphic correlation in western North America, which indicates that the Painted Desert Member of the Petrified Forest Formation (Bull Canyon equivalent) includes the late early Norian *Magnus* ammonite zone (Lucas 1991). The proposed correlation of the Redonda Formation with the late Sevatian pelagic sequence (Fig. 12) is rather tenuous. The possible Rhaetian age for the Redonda Formation (Hunt 1991) makes it permissible for these strata to be correlated with a younger part of the sequence, such as the upper k− zone of the Newark basin.

Data presented here are the first attempt to obtain a complete magnetostratigraphy for the Chinle Group; for that reason we regard our proposed correlations as preliminary. The reliability of the record needs to be further examined by testing its reproducibility, and more detailed sampling of mudstone-dominated sequences may improve its resolution. Greater resolution may be obtained by sampling additional sections on the Colorado plateau, which have received relatively little attention.

ACKNOWLEDGMENTS

Most of this research was supported by a post-doctoral fellowship from the Ford Foundation to Molina-Garza. We wish to thank Katerina Petronotis and Gary Acton for their help during sample collection. We also thank D. Kent for a detailed review and for making available to us a pre-print of magnetostratigraphic work of the Newark Supergroup, and G. Muttoni for making available a pre-print of magnetostratigraphic work of the Middle Triassic. We also thank A. Heckert for his assistance in the field.

REFERENCES

Ash, S.R., 1980. Upper Triassic floral zones of North America, in *Biostratigraphy of fossil plants, successional and paleoecological analysis,* pp. 153–170, eds Dilcher D.L. & Taylor T.N., Dowden, Hutchinson & Ross, Stroudsburg, PA.

Baag, C.G. & Helsley, C.E., 1974. Evidence of penecontemporaneous magnetization of the Moenkopi Formation, *J. geophys. Res.,* **79,** 3308–3320.

Bazard, D.R. & Butler, R.F., 1991. Paleomagnetism of the Chinle and Kayenta Formations, New Mexico and Arizona, *J. geophys. Res.,* **96,** 9847–9872.

Channell, J.E.T. & McCabe, C., 1994. Comparison of magnetic hysteresis parameters of unremagnetized and remagnetized limestones, *J. geophys. Res.,* **99,** 4613–4623.

Collinson, D.W., 1974. The role of pigment and specularite in the remanent magnetism of red sandstones, *Geophys. J. R. astr. Soc.,* **38,** 253–264.

Cornet, B., 1993. Applications and limitations of palynology in age, climatic, and paleoenvironmental analyses of Triassic sequences in North America, in *The nonmarine Triassic,* pp. 75–93, eds Lucas

S.G. & Morales M., New Mexico Museum of Natural History and Science Bulletin, **3,** 75–93.

Day, R., Fuller, M. & Schmidt, V.A., 1977. Hysteresis properties of titanomagnetites: grain-size and compositional dependence, *Phys. Earth. planet. Int.,* **13,** 260–267.

Ekstrand, E.J. & Butler, R.F., 1989. Paleomagnetism of the Moenave Formation: Implications for the Mesozoic North America apparent polar wander path, *Geology,* **84,** 1653–1655.

Elston, D.P. & Punicker, M.E., 1979. Detrital magnetization in red beds of the Moenkopi Formation (Triassic), Gray Mountain, Arizona, *J. geophys. Res.,* **84,** 1653–1665.

Fang, W. & Van der Voo, R., 1988. Paleomagnetism of Middle–Late Triassic plutons in southern Maine, *Tectonophysics,* **156,** 51–88.

Gallet, Y., Besse, J., Krystyn, L., Theveniaut, H. & Marcoux, J., 1993. Magnetostratigraphy of the Kavur Tepe section (southwest Turkey): A magnetic polarity time scale for the Norian, *Earth planet. Sci. Lett.,* **117,** 443–456.

Gallet, Y., Besse, J., Krystyn, L., Theveniaut, H. & Marcoux, J., 1994. Magnetostratigraphy of the Mayerling section (Austria) and Erenkolu Mezarlik (Turkey) section: Improvement of the Carnian (Late Triassic) magnetic polarity time scale, *Earth planet. Sci. Lett.,* **125,** 173–191.

Gallet, Y., Besse, J., Krystyn, L., Marcoux, J. & Theveniaut, H., 1992. Magnetostratigraphy of the Late Triassic Bolucektasi Tepe section (southwest Turkey): implications for changes in magnetic reversal frequency, *Phys. Earth planet. Inter.,* **73,** 85–108.

Grubbs, K.L. & Van der Voo, R., 1976. Structural deformation of the Idaho–Wyoming Overthrust Belt (U.S.A.), *Tectonophysics,* **33,** 321–336.

Haag, M. & Heller, F., 1991. Late Permian to Early Triassic magnetostratigraphy, *Earth planet. Sci. Lett.,* **107,** 42–54.

Harland, W.B., Armstrong, R.L., Cox, A.V., Craig, L.E., Smith, A.G. & Smith, D.F., 1990. A geologic Time Scale, Cambridge University Press, Cambridge.

Heller, F., Lowrie, W., Li, H. & Wang, J., 1988. Magnetostratigraphy of the Permian–Triassic boundary section at Shangsi (Guangyuan, Sichuan Province, China), *Earth planet. Sci. Lett.,* **88,** 348–356.

Helsley, C.E., 1969. Magnetic reversal stratigraphy of the Lower Triassic Moenkopi Formation of western Colorado, *Geol. Soc. Am. Bull.,* **80,** 2431–2450.

Helsley, C.E. & Steiner, M.B., 1974. Paleomagnetism of the Lower Triassic Moenkopi Formation, *Geol. Soc. Am. Bull.,* **85,** 457–464.

Herrera-Bervero, E. & Helsley, C.E., 1983. Paleomagnetism of a polarity transition in the Lower (?) Triassic Chugwater Formation, Wyoming, *J. geophys. Res.,* **88,** 3506–3522.

Huber, P., Lucas, S.G. & Hunt, A.P., 1993. Revised age and correlation of the Upper Triassic Chatham Group (Deep River basin, Newark Supergroup), North Carolina, Southeastern Geology, **33,** 171–193.

Hunt, A.P., 1991. Redonda Formation and Rock Point Member of the Chinle Formation (southwestern United States): are they Rhaetian (latest Triassic) in age, *Geol. Soc. Am. Abstr. with Prog.,* **23,** 35.

Hunt, A.P. & Lucas, S.G., 1991. The Paleorhinus biochron and the correlation of the nonmarine Triassic of Pangea, *Paleontology,* **34,** 487–501.

Kent, D.V. & Witte, W.K., 1993. Slow apparent polar wander for North America in the Late Triassic and large Colorado plateau rotation, *Tectonics,* **12,** 291–300.

Kent, D.V., Witte, W.K. & Olsen, P.E., 1995. Late Triassic–Earliest Jurassic geomagnetic polarity sequence and paleolatitudes from drill cores in the Newark rift basin, eastern North America, *J. Geophys. Res.,* **100,** 14965–14988.

Kirschvink, J.L., 1980. The least squares line and plane and the analysis of paleomagnetic data: examples from Siberia and Morroco, *Geophys. J. R. astr. Soc.,* **62,** 699–718.

Kodama, K.P., Cioppa, M.Y., Sherwood, E. & Warnock, A.C., 1994b. Paleomagnetism of baked sedimentary rocks in the Newark and Culpeper basins: Evidence for the J-1 cusp and significant Late Triassic apparent polar wander from the Mesozoic basins of North America, *Tectonics,* **13,** 917–928.

Kodama, K.P., Hedlund, C., Gosse, J. & Strasser, J., 1994a. Rotated paleomagnetic poles from the Sassamanville Syncline, Newark basin, southeastern Pennsylvania, *J. geophys. Res.,* **99,** 4643–4654.

Larrochelle, A. & Currie, K.L., 1967. Paleomagnetic studies of igneous rocks of the Manicouagan structure, Quebec, *J. geophys. Res.,* **72,** 4163–4169.

Larson, E.E., Walker, T.R., Patterson, P.E., Hoblitt, R.P. & Rosenbaum, J.G., 1982. Paleomagnetism of the Moenkopi Formation, Colorado plateau: basis for long-term model of acquisition of chemical remanent magnetism in red beds, *J. geophys. Res.,* **87,** 1081–1106.

Lienert, B.R. & Helsely, C.E., 1980. Magnetostratigraphy of the Moenkopi Formation at Bears Ears, Utah, *J. geophys. Res.,* **85,** 1475–1480.

Lowrie, W., Napoleone, G., Perch-Nielsen, K., Premoli-Silva, I. & Toumarkine, K., 1982. Paleogene magnetic stratigraphy in Umbrian pelagic carbonate rocks: The Contessa sections, Gubbio, *Geol. Soc. Am. Bull.,* **93,** 414–432.

Lucas, S.G., 1990. Towards a vertebrate biochronology of the Triassic, *Albertiana,* **8,** 36–41.

Lucas, S.G., 1991. Sequence stratigraphic correlation of nonmarine and marine Late Triassic biochronologies, western United States, *Albertiana,* **9,** 11–18.

Lucas, S.G., 1993. The Chinle Group: Revised stratigraphy and biochronology of Upper Triassic nonmarine strata in the western United States, in *Aspects of Mesozoic geology and paleontology of the Colorado plateau,* pp. 27–50, ed. Morales M., Museum of northern Arizona Bull., **59**.

Lucas, S.G., 1995. The Triassic Sinbad Formation and correlation of the Moenkopi Group, Canyonlands National Park, Utah, in *National Park Service Paleontological Research,* p. 54–57, eds Santucci, V. & McClelland, L., Natural Resources Publication Office, Denver.

Lucas, S.G. & Hunt, A.P., 1987. Stratigraphy of the Anton Chico and Santa Rosa Formations, Triassic of east-central New Mexico, *J. Arizona–Nevada Acad. Sci.,* **22,** 21–33.

Lucas, S.G. & Hunt, A.P., 1989. Revised stratigraphy in the Tucumcari basin, east-central New Mexico, in *Dawn of the age of the dinosaurs in the American southwest,* pp. 150–170, eds Lucas, S.G. & Hunt, A.P., New Mexico Museum of Natural History.

Lucas, S.G. & Hunt, A.P., 1993. Tetrapod biochronology of the Chinle Group (Upper Triassic), western United States, in *The nonmarine Triassic,* pp. 327–329, eds Lucas, S.G. & Morales, M., New Mexico Museum of Natural History & Sci. Bull., **3**.

Lucas, S.G. & Morales, M., 1985. Middle Triassic amphibian, in *Santa Rosa–Tucumcari Region,* pp. 56–58, eds Lucas, S.G. & Zidek, J., New Mexico Geol. Soc. Guidebook 36, University of New Mexico Press, Albuquerque.

Lucas, S.G., Hunt, A.P. & Huber, P., 1990. Triassic stratigraphy in the Sangre de Cristo Mountains: New Mexico. *New Mexico Geol. Soc. Guidebook* **41,** 305–318.

McFadden, P.L. & McElhinny, 1990. Classification of the reversal test in paleomagnetism, *Geophys. J. Int.,* **103,** 725–729.

McIntosh, W.C., Hargraves, R.B. & West, C.L., 1985. Paleomagnetism and oxide mineralogy of Upper Triassic to Lower Jurassic red beds and basalts in the Newark Basin. *Geol. Soc. Am. Bull.,* **96,** 463–480.

McMahon, B.E. & Strangway, D.W., 1968. Stratigraphic implications of paleomagnetic data from Upper Paleozoic-Lower Triassic redbeds of Colorado. *Geol. Soc. Am. Bull.,* **79,** 417–428.

Molina-Garza, R.S., Geissman, J.W. & Lucas, S.G., 1993. Late Carinian–early Norian magnetostratigraphy from nonmarine strata, Chinle Group, New Mexico. Contributions to the Triassic magnetic polarity time scale and the correlation of nonmarine and marine Triassic faunas, in *The nonmarine Triassic,* pp. 345–352, eds Lucas, S.G. & Morales, M., New Mexico Museum of Natural History & Sci. Bull., **3**.

Molina-Garza, R.S., Geissman, J.W. & Van der Voo, R., 1995. Paleomagnetism of the Dockum Group (Upper Triassic), northwest Texas: Further evidence for the J-1 cusp in the North America APWP and implications for Colorado plateau rotation and rate of Triassic APW, *Tectonics,* **14,** 979–993.

Molina-Garza, R.S., Geissman, J.W., Van der Voo, R., Lucas, S.G. & Hayden, S., 1991. Paleomagnetism of the Moenkopi and Chinle Formations in central New Mexico: Implications for the North American apparent polar wander path and Triassic magnetostratigraphy, *J. geophys. Res.,* **96,** 14 239–14 262.

Morales, M., 1987. Terrestrial fauna and flora from the Triassic Moenkopi Formation of the southwestern United States, *J. Arizona–Nevada Acad. Sci.,* **22,** 1–19.

Morales, M., 1993. Tetrapod biostratigraphy of the lower-middle Triassic Moenkopi Formation, in *The nonmarine Triassic,* pp. 355–358, eds Lucas, S.G. & Morales, M., New Mexico Museum of Natural History & Sci. Bull., **3.**

Muttoni, G. & Kent, D.V., 1994. Paleomagnetism of latest Anisian (Middle Triassic) sections of the Prezzo Limestone and Buchtenstein Formation, southern Alps, Italy, *Earth planet. Sci. Lett.,* **122,** 1–18.

Muttoni, G., Channel, J.E.T., Nicora, A. & Rettori, R., 1994. Magnetostratigraphy and biostratigraphy of an Anisian–Ladinian (Middle Triassic) boundary section from Hydra (Greece), *Palaeogeog. Palaeoclimat. Palaeoecol.,* **111,** 249–262.

Ogg, J.G. & Steiner, M.B., 1991. Early Triassic magnetic polarity time scale-integration of magnetostratigraphy, ammonite zonation and sequence stratigraphy from stratotype sections (Canadian Artic Archipelago), *Earth planet. Sci. Lett.,* **107,** 69–89.

Olsen, P.E., 1986. A 40-million-year lake record of early Mesozoic orbital climatic forcing, *Science,* **234,** 842–848.

Picard, M.D., 1964. Paleomagnetic correlation of units within Chugwater (Triassic) Formation, west–central Wyoming, *Bull. Am. Assoc. Petrol. Geol.,* **48,** 269–291.

Purucker, M.D., Elston, D.P. & Shoemaker, E.M., 1980. Early acquisition of characteristic magnetization in red beds of the Moenkopi Formation (Triassic), Gray Mountain, Arizona, *J. geophys. Res.,* **85,** 997–1012.

Reeve, S.C., 1985. Paleomagnetic studies of sedimentary rocks of Cambrian and Triassic age, *PhD Thesis,* University of Texas at Dallas, TX.

Reeve, S.C. & Helsley, C.E., 1972. Magnetic reversal sequence in the upper portion of the Chinle Formation, Montoya, New Mexico. *Geol. Soc. Am. Bull.,* **83,** 3795–3812.

Shive, P.N., Steiner, M.B. & Huycke, D.T., 1984. Magnetostratigraphy, paleomagnetism, and remanence acquisition in the Triassic Chugwater Formation of Wyoming, *J. geophys. Res.,* **89,** 1801–1815.

Shoemaker, E.M. & Newman, W.L., 1959. Moenkopi Formation (Triassic? and Triassic), in Salt Anticline region, Colorado and Utah, *Am. Assoc. Petrol. Geol. Bull.,* **43,** 1835–1851.

Smith, W.A., 1987. Paleomagnetic results from a crosscutting system of northwest and north–south trending diabase dikes in the North Carolina Piedmont, *Tectonophysics,* **136,** 137–150.

Steiner, M.B., 1986. Rotation of the Colorado plateau, *Tectonics,* **5,** 649–660.

Steiner, M.B. & Lucas, S.G., 1992. A Middle Triassic paleomagnetic pole for North America, *Geol. Soc. Am. Bull.,* **104,** 993–998.

Steiner, M.B., Morales, M. & Shoemaker, E.M., 1993. Magnetostratigraphic, biostratigraphic and lithologic correlations in Triassic strata of the western U.S., in *Applications of Paleomagnetism to Sedimentary Geology,* Spec. Publ. 49, pp. 41–58, eds Aissaoui, D.M., McNeill, D.F. & Hurley, N.F., SEPM, Tulsa, OK.

Steiner, M.B., Ogg, J.G., Zhang, Z. & Sun, S., 1989. The Late Permian/Early Triassic magnetic polarity time scale and plate motions of South China. *J. geophys. Res.,* **94,** 7343–7363.

Stewart, J.H., Poole, F.G. & Wilson, R.F., 1972. Stratigraphy and origin of the Chinle Formation and related Upper Triassic strata in the Colorado plateau region, US Geol. Surv. Prof. Pap., **690.**

Symons, D.T.A., Bormann, R.E. & Jans, R.P., 1989. Paleomagnetism of Triassic redbeds of the lower Fundy Group and Mesozoic tectonism of the Nova Scotia platform, Canada, *Tectonophysics,* **164,** 13–24.

Van der Voo, R., 1990. Phanerozoic paleomagnetic poles from Europe and North America and comparisons with continental reconstructions, *Rev. Geophys.,* **28,** 167–206.

Van der Voo, R. & Grubbs, K.L., 1977. Paleomagnetism of the Chugwater redbeds revisited (Wyomings, U.S.A.), *Tectonophysics,* **44,** T27–T33.

Van Fossen, M.C., Flynn, J.J. & Forsythe, R.D., 1986. Paleomagnetism of Early Jurassic rocks, Watchung Mountains, Newark Basin: evidence for complex rotation along the border fault, *Geophys. Res. Lett.,* **13,** 185–188.

Van Houten, F.B., 1962. Cyclic sedimentation and the origin of analcime-rich Upper Triassic Lockatong Formation, west-central New Jersey and adjacent Pennsylvania, *Am. J. Sci.,* **260,** 561–576.

Witte, W.K. & Kent, D.V., 1989. A middle Carnian to early Norian (225Ma) paleopole from sediments of the Newark Basin, Pennsylvania, *Geol. Soc. Am. Bull.,* **101,** 1118–1126.

Witte, W.K. & Kent, D.V., 1990. The paleomagnetism of red beds and basalts of the Hettangian extrusive zone, Newark Basin, New Jersey, *J. geophys. Res.,* **95,** 17 533–17 545.

Witte, W.K., Kent, D.V. & Olsen, P.E., 1991. Magnetostratigraphy and paleomagnetic poles from Late Triassic–earliest Jurassic strata of the Newark Basin, *Geol. Soc. Am. Bull.,* **103,** 1648–1662.

Zijderveld, J.D.A., 1967. A.C. demagnetization of rocks: Analysis of results, in *Methods in rock magnetism and paleomagnetism,* pp. 254–286, eds Collison, D.W., Creer, K.M. & Runcorn, S.K., Elsevier, Amsterdam.